Soil Dynamics and Earthquake Engineering 176 (2024) 108267

Contents lists available at ScienceDirect

Soil Dynamics and Earthquake Engineering

journal homepage: www.elsevier.com/locate/soildyn

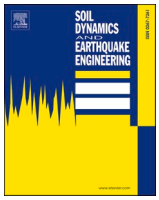

Insights from liquefaction ejecta case histories for the 2010–2011 Canterbury earthquakes

Zorana Mijic [a,*], Jonathan D. Bray [b]

[a] Depart. of Civil, Construction, and Environmental Engineering, The Pennsylvania State Univ., USA
[b] Depart. of Civil and Environmental Engineering, Univ. of California, Berkeley, USA

ARTICLE INFO

Keywords:
Case histories
Ejecta
Ground failure
Liquefaction
Settlement

ABSTRACT

A database of detailed liquefaction ejecta case histories for the 2010–2011 Canterbury earthquakes is interrogated. More than 50 mm of ejecta-induced settlement occurred at thick, clean sand sites shaken by $PGA_{6.1}$ = 0.35–0.70 *g* (wherein $PGA_{6.1}$ is the peak ground acceleration for a M_w 6.1 earthquake), whereas ejecta-induced settlement at highly stratified silty soil sites did not exceed 10 mm even when $PGA_{6.1}$ exceeded 0.45 *g*. Cone penetration test-based liquefaction-induced damage indices that do not consider soil-system response effects, such as post-shaking hydraulic mechanisms, overestimate the severity of ejecta at stratified silty soil sites. Considering post-shaking hydraulic mechanisms captures the lack of ejecta at stratified silty soil sites. It also improves the estimation of ejecta severity at clean sand sites with severe-to-extreme ejecta. Strongly shaken clean sand sites that did not produce ejecta typically had thick strata with high tip resistances, thick non-liquefiable crusts, or deeper non-liquefiable strata overlying liquefiable strata. Ejecta-induced fissures formed in the non-liquefiable crust during the Feb 2011 earthquake which liquefied soil at depth could exploit to produce ejecta during the Jun 2011 earthquake. When significant ejecta formed on the roads, elevated adjacent ground with houses typically had negligible ejecta.

1. Introduction

Sediment ejecta, as one of the key effects of earthquake-induced liquefaction, have the potential to cause substantial damage to the land and infrastructure. The main 2010–2011 Canterbury, New Zealand, earthquakes (i.e., 4 Sep 2010 M_w 7.1, 22 Feb 2011 M_w 6.2, 13 Jun 2011 M_w 6.2, and 23 Dec 2011 M_w 6.1 events) triggered widespread, damaging liquefaction throughout Christchurch and its suburbs (e.g., Refs. [1,2]). Approximately 51,000 of 140,000 residential properties were affected by liquefaction [3]. The level of liquefaction ejecta-induced damage varied from site to site and from earthquake to earthquake. The Feb 2011 earthquake caused the most severe and widespread liquefaction ejecta. Compared to the rest of Christchurch, residential areas to the east of the Central Business District (CBD) experienced the most severe effects of liquefaction due to the intense ground shaking, shallow groundwater table, and soil deposits that are more susceptible to liquefaction triggering and manifestations (e.g., Refs. [1,4]).

The occurrence and severity of surficial liquefaction manifestation is commonly estimated using liquefaction-induced ground failure indices in conjunction with simplified stress-based liquefaction triggering procedures. The liquefaction potential index (LPI) proposed by Iwasaki et al. [5] considers the influence of the liquefiable layer thickness and its proximity to the ground surface, as well as the soil's relative density (D_r) through the factor of safety against liquefaction triggering (FS_L), on the severity of liquefaction manifestation at the ground surface. However, LPI does not explicitly account for the influence of contractive/dilative tendencies of soil and the thickness of a non-liquefiable layer immediately below the ground surface (i.e., crust) on the severity of liquefaction manifestation. The liquefaction severity number (LSN) developed by van Ballegooy et al. [6] incorporates the Ishihara and Yoshimine [7] post-liquefaction volumetric strain relationship based on FS_L and D_r to account explicitly for the soils' contractive/dilative tendencies. Additionally, LSN employs a hyperbolic depth-weighting function to emphasize the importance of crust thickness on the severity of liquefaction manifestation. Although not a numerical index, the Ishihara [8] boundary curves for different peak ground acceleration (PGA) values separate sites with and without surficial manifestation of liquefaction based on the relative thicknesses of the non-liquefiable crust and an underlying liquefiable soil layer. His work is based on sites with and

* Corresponding author. The Pennsylvania State University, W236 Olmsted Building, Middletown, PA, 17057, USA.
E-mail address: zorana.mijic@psu.edu (Z. Mijic).

https://doi.org/10.1016/j.soildyn.2023.108267
Received 22 July 2023; Received in revised form 22 September 2023; Accepted 23 September 2023
Available online 12 October 2023

without surficial manifestation of liquefaction in two earthquakes. Hutabarat and Bray [9] incorporated the depth of liquefaction triggering, soil stratification, and vertical hydraulic conductivity as governing factors in the occurrence and severity of surficial liquefaction manifestation using the liquefaction ejecta demand (L_D) and crust layer resistance (C_R) parameters. These two parameters account for soil-system response effects (e.g., post-shaking hydraulic mechanisms) not captured by the previously mentioned liquefaction-induced damage indices [10]. All liquefaction indices would benefit from additional validation from field case histories.

None of the existing liquefaction-induced damage indices can directly quantitatively estimate the settlement due to ejecta. Nonlinear effective stress analysis can calculate the excess hydraulic head and the Ejecta Potential Index (EPI) to estimate the severity of ejecta [11]; however, it may not be feasible to conduct the advanced analysis when subsurface data and ground motion recordings are limited. Moreover, effective-stress models can capture the settlement caused by two of the three liquefaction-induced displacement mechanisms (i.e., volumetric- and shear-induced mechanisms) but continuum-based approaches cannot capture the ejecta-induced mechanism [12]. Thus, even advanced analyses are not a viable means to directly estimate ejecta-induced settlement.

To improve the understanding of the liquefaction ejecta phenomenon, Mijic et al. [13] developed the first liquefaction ejecta database comprised of detailed case histories for 58 free-field, level-ground sites shaken by the four main Canterbury earthquakes and three additional sites for only the Sep 2010 earthquake because lateral spreading occurred during the Feb 2011 earthquake. They estimated the ejecta-induced settlement with access to the comprehensive T + T [14] and LDAT [15] databases because direct measurements of ejecta and associated free-field damage had not been conducted after the Canterbury earthquakes. They employed photographic evidence and LiDAR surveys to estimate the free-field ejecta-induced settlement. The Mijic et al. [13] database also contains the information about PGA, groundwater depth, soil profile, crust thickness, liquefiable layer thickness, and liquefaction-induced damage indices such as LSN, LPI, and L_D-C_R for each case history.

Considering the importance of field case histories for advancing the state of knowledge and practice in geotechnical earthquake engineering, the interrogation of the Mijic et al. [13] database to better understand the formation and effects of liquefaction ejecta and to advance the state of practice as it relates to the liquefaction ejecta phenomenon is warranted. In this paper, factors that could contribute to the manifestation of ejecta and differing amounts of ejecta-induced settlement from site to site and from earthquake to earthquake are examined. The observed ejecta-induced settlement is also compared with several of the existing liquefaction severity indices.

2. Overview of the liquefaction ejecta database

2.1. Site geology

Christchurch is situated in the northern Canterbury Plains, just north of the Port Hills of Banks Peninsula, an extinct volcanic complex on the eastern shore of the South Island, New Zealand. Due to the complexity of depositional environment, four geologic quadrants centered on the CBD – southwest (SW), northwest (NW), northeast (NE), and southeast (SE) – can be identified [4]. The main characteristics of the SW quadrant are thick successions of thinly interbedded fine sand and silt swamp deposits and the influence of the Port Hills on the depositional setting. The NW quadrant, too, is comprised of silty soil swamp deposits; however, it lacks depositional effects from the Port Hills and likely contains younger sediments than the SW quadrant as well as thicker sand strata and thinner silt strata than the SW quadrant. The NE and SE quadrants are characterized by interchanging layers of coastal and fluvial sediments and thicker layers of clean sand [4].

The Mijic et al. [13] liquefaction ejecta database contains nine, eight, four, and 40 sites with detailed case histories in the SW, NW, SE, and NE quadrants, respectively. Most sites are in the NE quadrant due to the predominance of ejecta-induced land and lightweight house damage in this quadrant. Considering the complexity of liquefaction phenomenon and the depositional Christchurch environment, localized geology, as well as the simplified conventional methodologies for liquefaction assessment, four soil deposit categories were used for Christchurch [13]. Thick, clean sand deposits (Category 1) are characterized by at least 3-m thick sand layer below the groundwater table in the top 10 m of the soil profile, while highly stratified silty soil deposits (Category 3) do not have a sand layer thicker than 1 m below the groundwater table in the top 10 m of the soil profile. Partially stratified silty soil deposits belong to Category 2 and have a sand stratum between 1 m and 3 m in thickness below the groundwater table in the top 10 m of the soil profile. Lastly, gravel-dominated soil deposits (Category 4) are characterized by at least 3-m thick gravel layer below the groundwater table in the top 10 m of the soil profile. A layer was considered continuous if it was not interrupted by a layer of different soil type that was more than 200-mm thick. The available CPT profiles in combination with borehole logs were used to classify a soil deposit at each of the 61 sites. The CPT soil behavior type index (I_c, [16]) thresholds of 1.3 and 1.8 were used to distinguish between gravelly soil and clean sand and between clean sand and fines-containing sand, respectively. There are 42 thick, clean sand sites, nine partially stratified silty soil sites, six highly stratified silty soil sites, and four gravel-dominated sites. Their distribution among the four geologic quadrants is summarized in Table 1.

These soil deposit category definitions are more detailed than the ones used in the Hutabarat and Bray [9] numerical study wherein a sand layer of 4.5 m in thickness was used as a boundary between a thick, clean sand deposit and a stratified silty soil deposit. Changing the threshold thickness in this study from 3 m to 4.5 m would not likely change the following analyses significantly because the thickness of a clean sand layer alone is not the only important factor in the identification of a critical soil layer responsible for the manifestation of liquefaction at the ground surface. The liquefaction resistance and the position of the sand layer within a soil profile are also important for the assessment of the critical layer (e.g., Ref. [17]).

2.2. Liquefaction ejecta-induced settlement estimates

The liquefaction ejecta-induced free-field, level-ground settlement was estimated by Mijic et al. [13] at 61 sites for 10-, 20-, and 50-m radial areas (herein called buffers) for up to four earthquakes of the 2010–2011 Canterbury earthquake sequence. The settlement assessment area within each buffer typically contained at least one CPT and depended on the presence of dwellings, vegetation, human-made alterations of the natural and built environment, and similar factors that had the potential to obscure ejecta or affect the photographic evidence and LiDAR surveys [13]. Sites in an open field (e.g., parks and playgrounds) typically had a large portion of each buffer assessed for ejecta-induced settlement, whereas sites at residential properties typically had one to three open patches of their properties and adjacent roads considered for the evaluation of ground settlement due to ejecta.

Table 1
Distribution of soil deposit categories across the geologic quadrants.

Quadrant	Number of sites per soil deposit category			
	Thick, clean sand (Category 1)	Partially stratified (Category 2)	Highly stratified (Category 3)	Gravel-dominated (Category 4)
NE	38	2	0	0
SE	3	1	0	0
NW	0	3	3	2
SW	1	3	3	2

The ejecta-induced settlement at each site for each earthquake was evaluated by Mijic et al. [13] using the photographic-based approach only or the photographic-based approach in combination with the LiDAR-based approach (the weighted average of the two estimates). The photographic-based approach involved the use of aerial and ground photographs, detailed property inspection reports and maps, and geometrical approximations of the ejected soil shapes. The alternative approach was based on LiDAR point elevations and one-dimensional, free-field volumetric-induced settlement for level ground estimated using the Zhang et al. [18] procedure. Ejecta-induced settlement was estimated by subtracting the volumetric-induced settlement estimate from the total liquefaction-induced settlement measured using pre- and post-earthquake LiDAR surveys. Shear-induced settlement was neglected because the case histories represented free-field sites (i.e., no structures or only light-weight structures were near the center of the site). The weighted average of the photographic- and LiDAR-based estimates provided the best estimate of the free-field ejecta-induced settlement [13]. For a settlement assessment area, the areal ejecta-induced ground settlement was calculated as the ratio of the total volume of ejecta to the total assessment area. The localized ejecta-induced settlement (calculated by dividing the total volume of ejecta with only the area covered by ejecta) was also estimated by Mijic et al. [13] due to its importance for the assessment of differential building settlement. The localized ejecta-induced settlement is generally higher than the areal ejecta-induced settlement because it does not incorporate the areal averaging.

Mijic et al. [13] analyzed 58 sites for all four main Canterbury earthquakes and three sites for the Sep 2010 earthquake, as noted previously. All four main Canterbury earthquakes were considered in this study due to the availability and similar quality of the data used to estimate the ejecta-induced settlement. Typically, three areal buffers and more than one assessment area were analyzed for each site to develop one representative value (best estimate) of the ejecta-induced settlement at a site for each earthquake, which produced 235 case histories in total. Only the best estimates of free-field ejecta-induced settlement are discussed in this paper for brevity.

Fig. 1 illustrates the distribution of ejecta-induced settlement values for each of the four main earthquake events. The Sep 2010 dataset contains the representative settlement values at 61 sites, while each of the Feb 2011, Jun 2011, and Dec 2011 datasets consists of representative settlement values at 58 sites. Having three extra case histories in the Sep 2010 dataset has a negligible impact on its ejecta-induced settlement range and median; thus, they are included in the following discussion. The ranges of the Sep 2010, Feb 2011, Jun 2011, and Dec 2011 ejecta-induced settlement values are 0–40 mm, 0–155 mm, 0–105 mm, and 0–120 mm, respectively, while the respective median ejecta-induced settlements are 0 mm, 35 mm, 10 mm, and 0 mm. As a comparison, the median localized ejecta-induced settlement values for the Sep 2010, Feb 2011, Jun 2011, and Dec 2011 earthquakes are 0 mm, 50 mm, 20 mm, and 0 mm, respectively, while the respective ranges are 0–70 mm, 0–200 mm, 0–105 mm, and 0–120 mm. The median values of the localized-to-areal ejecta-induced settlement ratios are 2.4, 1.2, 1.6, and 3.0 for the Sep 2010, Feb 2011, Jun 2011, and Dec 2011 earthquakes, respectively. The settlement values are rounded to the nearest 5 mm in this study to make comparisons. They should be rounded off to the nearest 10 mm when used in practice due to the inherent uncertainty in estimating ejecta-induced settlement.

The ejecta-induced settlement can be grouped in five categories – none (0 mm), minor (1–25 mm), moderate (26–50 mm), severe (51–100 mm), and extreme (>100 mm). In the paper, *zero* and *non-zero* are used at times to distinguish between the none ejecta-induced settlement category and the categories with minor, moderate, severe, and extreme ejecta-induced settlement. Among the four earthquakes, the number of common sites that did not produce ejecta-induced settlement is the greatest for the Sep 2010 earthquake (53 sites) and the lowest for the Feb 2011 earthquake (15 sites), as shown in Fig. 2. The greatest number of sites with severe-to-extreme ejecta-induced settlement corresponds to the Feb 2011 earthquake (21 sites), while no sites with severe-to-extreme ejecta-induced settlement are identified for the Sep 2010 event. There are 44 and 54 sites that underwent none-to-minor ejecta-induced settlement in the Jun 2011 and Dec 2011 earthquakes, respectively. There are only five and three sites with severe-to-extreme ejecta in the Jun 2011 and Dec 2011 earthquakes, respectively. Lastly, 14 sites did not produce ejecta in any of the four earthquakes.

3. Effects of ground motion and site characteristics on ejecta-induced settlement

The relationships between the liquefaction ejecta-induced settlement and parameters available in the Mijic et al. [13] database are examined for 44 sites that generated ejecta in at least one of the four main Canterbury earthquakes (176 case histories). The effects of PGA, soil profile, groundwater depth, crust thickness, and liquefiable layer thickness on the amount of settlement due to ejecta are investigated. The relationships between these variables and the ejecta-induced settlement are

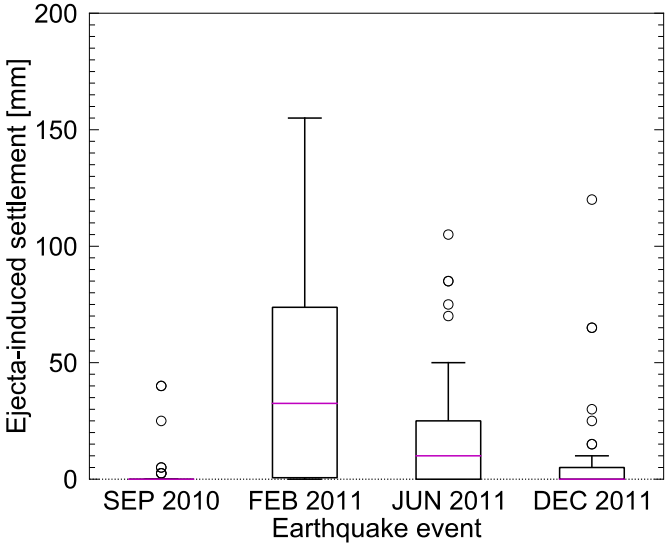

Fig. 1. Box and whiskers showing distribution of ejecta-induced settlement for each of the four main Canterbury earthquakes (magenta = median).

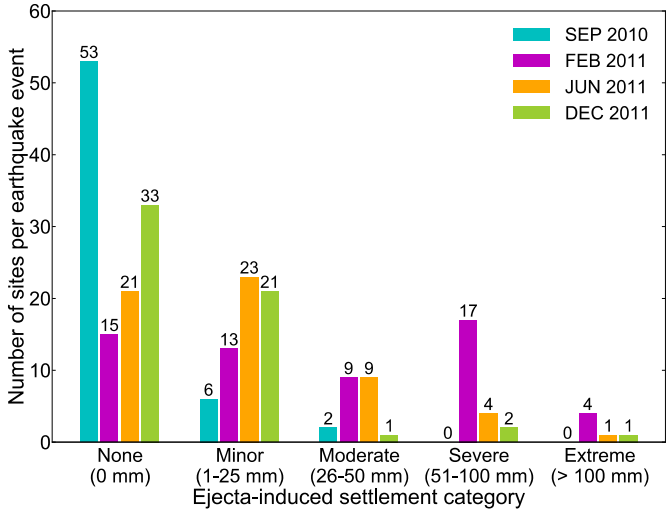

Fig. 2. The number of sites per liquefaction ejecta-induced settlement category for each of the four main Canterbury earthquakes.

explored using Spearman's correlation coefficient (R_S), which is mathematically equivalent to Pearson's correlation coefficient for the ranked data. The choice stems primarily from the distribution of the data, which is not always normal, and the possibility of having variables that are associated nonlinearly. In theory, the correlation coefficient definition applies only to the bivariate normal distribution of two variables [19]. Spearman's correlation coefficient does not require the jointly normally distributed data and can measure a monotonic association between two variables [20,21]. The strength of the correlation in this study is described as very weak, weak, moderate, strong, and very strong if the absolute value of R_S = 0.00–0.19, 0.20–0.39, 0.40–0.59, 0.60–0.79, and 0.80–1.0, respectively. The complexity of the formation of ejecta due to the variability in earthquake ground motions and site conditions, and factors such as the presence of cracks in the crust, uncertainty in estimating ejecta-induced settlement, and the inability to control variables in the natural setting complicate the interpretation of the dependence of ejecta-induced settlement on parameters such as PGA, groundwater depth, and crust and liquefiable layer thicknesses.

3.1. Peak ground acceleration

PGA is commonly used in simplified liquefaction triggering procedures to evaluate the seismic demand on soil (cyclic stress ratio, CSR) and thereby the FS_L. The median PGA for each of the four main Canterbury earthquakes was estimated by Bradley and Hughes [22,23]. These values are provided in Mijic et al. [13] for each liquefaction ejecta case history. The range of the median PGA values at the 44 sites is 0.17–0.31 *g*, 0.32–0.68 *g*, 0.13–0.43 *g*, and 0.12–0.37 *g* for the M_w 7.1 Sep 2010, M_w 6.2 Feb 2011, M_w 6.2 Jun 2011, and M_w 6.1 Dec 2011 events, respectively. The medians of these median PGA values for the respective earthquakes are 0.19 *g*, 0.43 *g*, 0.24 *g*, and 0.29 *g*. The distribution of sites with different levels of ejecta-induced settlement relative to PGA being ≤ 0.20 *g*, 0.21–0.30 *g*, 0.31–0.40 *g*, and > 0.40 *g* is illustrated in Fig. 3 for each of the four main Canterbury earthquakes. In general, there appears to be a tendency for the ejecta-induced settlement to decrease as the PGA decreases.

To compare the settlement among the four earthquakes with different M_w, the Bradley and Hughes [22,23] PGA values are scaled to an equivalent M_w 6.1 earthquake (the lowest M_w of the four earthquakes) using the Idriss and Boulanger [24] magnitude scaling factor (MSF = 6.9*exp(-M_w/4) - 0.058 ≤ 1.8). The original PGA for the Sep 2010, Feb 2011, and Jun 2011 earthquakes are multiplied by 1.30, 1.03, and 1.03, respectively, to obtain the magnitude-weighted PGA, hereinafter referred to as $PGA_{6.1}$. The Feb 2011 earthquake is generally characterized by the most intense $PGA_{6.1}$ (median = 0.44 *g*, range = 0.33–0.70 *g*) compared to the Sep 2010, Jun 2011, and Dec 2011 $PGA_{6.1}$ (median = 0.25 *g*, 0.24 *g*, and 0.29 *g*, respectively, and range = 0.22–0.40 *g*, 0.13–0.44 *g*, and 0.12–0.37 *g*, respectively). This is consistent with the observations of the greatest number of sites with severe-to-extreme liquefaction ejecta-induced settlement for the Feb 2011 earthquake (21 sites), which were all triggered by $PGA_{6.1} \geq 0.35$ *g*. Conversely, there are no sites with severe-to-extreme ejecta-induced settlement for the Sep 2010 earthquake.

The ejecta-induced settlement generally tends to increase as $PGA_{6.1}$ increases (Fig. 4), as one would expect. However, there is much scatter. The median settlement values for the case histories in the $PGA_{6.1} \leq 0.20$ *g*, 0.21–0.30 *g*, 0.31–0.40 *g*, and >0.40 *g* groups are 0 mm, < 5 mm, 15 mm, and 55 mm, respectively. Spearman's correlation coefficient of 0.56 also indicates a positive moderate correlation between the ejecta-induced settlement and $PGA_{6.1}$ for all 176 case histories together. The $PGA_{6.1} \leq 0.20$ *g* case histories correspond to the Jun 2011 and Dec 2011 earthquakes and are predominantly with zero ejecta-induced settlement. Only 20% (3/15) of the $PGA_{6.1} \leq 0.20$ *g* case histories have non-zero ejecta-induced settlement, which does not exceed 15 mm. Nearly one-

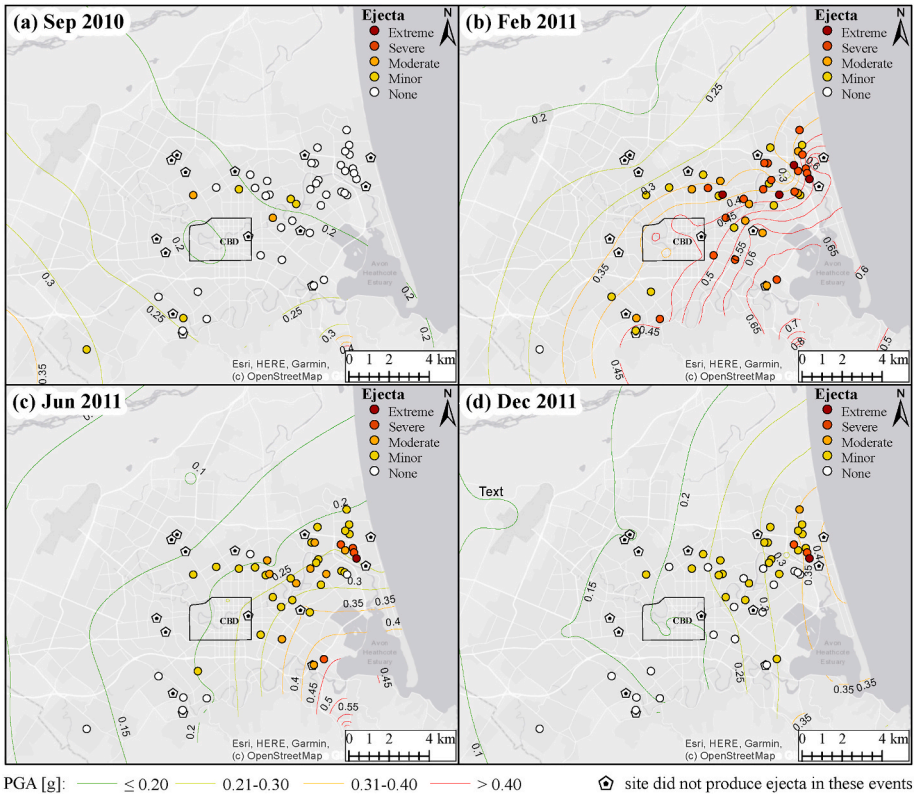

Fig. 3. Distribution of 44 sites relative to the Bradley and Hughes [22,23] median PGA contours for the (a) Sep 2010, (b) Feb 2011, (c) Jun 2011, and (d) Dec 2011 earthquakes. The ejecta-induced settlement experienced at each site is shown as none (0 mm), minor (1–25 mm), moderate (26–50 mm), severe (51–100 mm), and extreme (> 100 mm). Fourteen sites that did not produce ejecta in any of the four earthquakes are also shown.

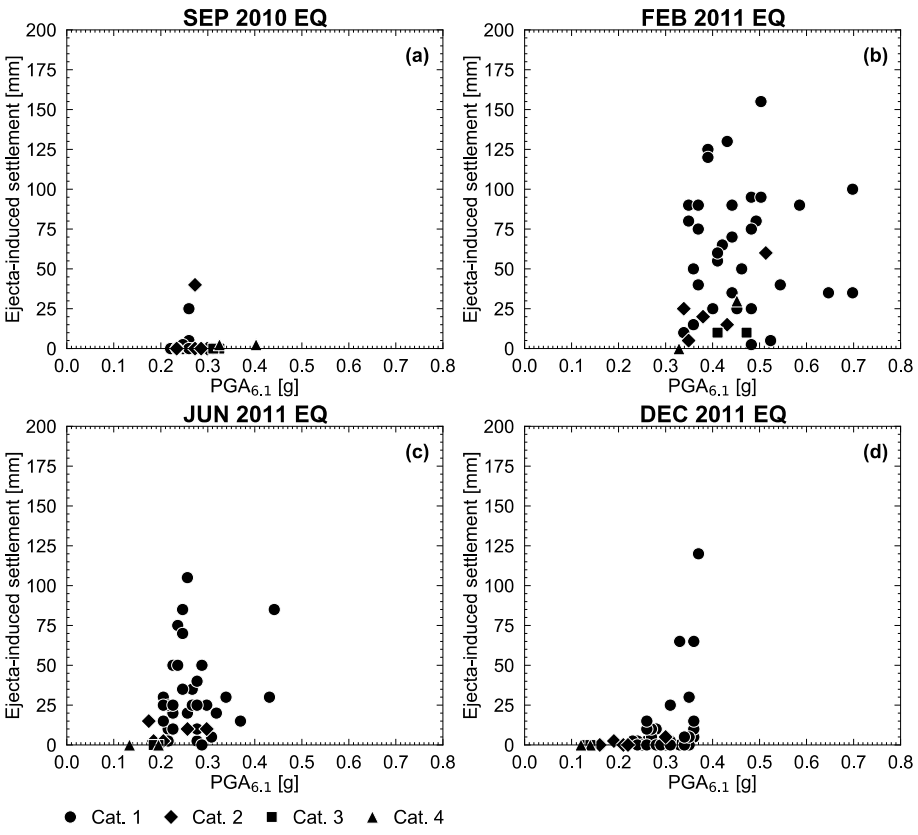

Fig. 4. Ejecta-induced settlement versus $PGA_{6.1}$ for (a) Sep 2010 earthquake ($R_S = 0.32$), (b) Feb 2011 earthquake ($R_S = 0.18$), (c) Jun 2011 earthquake ($R_S = 0.43$), and (d) Dec 2011 earthquake ($R_S = 0.54$). Different site categories (Cat. 1 = thick, clean sand, Cat. 2 = partially stratified, Cat. 3 = highly stratified, and Cat. 4 = gravel-dominated) are represented by different symbols.

half (43/89) of the $PGA_{6.1} = 0.21$–0.30 *g* case histories are with zero ejecta-induced settlement and correspond mostly to the Sep 2010 earthquake. About 60% of non-zero ejecta case histories in this $PGA_{6.1}$ group, including four severe-to-extreme ejecta-induced settlement case histories, correspond to the Jun 2011 earthquake. This $PGA_{6.1}$ group's non-zero ejecta case histories for the Sep 2010 and Dec 2011 earthquakes have up to 40 mm and 15 mm of ejecta-induced settlement, respectively. The median ejecta-induced settlement for the Sep 2010, Jun 2011, and Dec 2011 earthquake case histories are 0 mm, 25 mm, and $<$ 5 mm, respectively. Of 41 case histories in the $PGA_{6.1} = 0.31$–0.40 *g* group, 22% have no ejecta-induced settlement, while 46%, 10%, and 22% have minor, moderate, and severe-to-extreme ejecta-induced settlement, respectively. The no-ejecta case histories correspond to the Sep 2010 and Dec 2011 earthquakes (apart from one case history for the Feb 2011 earthquake) and the 0.31–0.35 *g* $PGA_{6.1}$ range, whereas the severe-to-extreme ejecta case histories correspond to the Feb 2011 and Dec 2011 earthquakes and the 0.33–0.39 *g* $PGA_{6.1}$ range. In case of $PGA_{6.1} > 0.40$ *g*, 0%, 22%, 26%, and 52% of 31 case histories have none, minor, moderate, and severe-to-extreme ejecta-induced settlement, respectively. Ninety-four percent of these severe-to-extreme ejecta case histories correspond to the Feb 2011 earthquake.

The no-ejecta case histories in the $PGA_{6.1} \leq 0.20$ *g* group are represented by all four site categories, while the three minor ejecta case histories (up to 15 mm of ejecta-induced settlement) in the $PGA_{6.1} \leq 0.20$ *g* group are from partially stratified silty soil deposits. In the $PGA_{6.1} = 0.31$–0.40 *g* group, both the zero and non-zero ejecta case histories are characterized primarily by thick, clean sand deposits (67% and 84%, respectively). Similarly, most non-zero ejecta case histories in the $PGA_{6.1} > 0.40$ *g* group correspond to thick, clean sand deposits (84%). Case histories with $PGA_{6.1} > 0.40$ *g* that are characterized by highly stratified, partially stratified, and gravel-dominated sites generated up to 10 mm ($PGA_{6.1} = 0.47$ *g*), 60 mm ($PGA_{6.1} = 0.51$ *g*), and 30 mm ($PGA_{6.1} = 0.45$ *g*) of ejecta-induced settlement, respectively.

Overall, the severe-to-extreme ejecta case histories occur for higher $PGA_{6.1}$ values in the Feb 2011, Jun 2011, and Dec 2011 earthquakes (i.e., 0.35–0.70 *g*, 0.24–0.44 *g*, and 0.33–0.37 *g*, respectively). The severe-to-extreme ejecta case histories are thick, clean sand deposits in 97% of the cases (28/29). The no-ejecta case histories exist for $PGA_{6.1} \leq 0.35$ *g* and for all site categories. Additionally, these lower levels of shaking did not produce ejecta in the Sep 2010 earthquake at most sites, which are predominantly thick, clean sand deposits. However, most of the same sites produced ejecta in the Jun 2011 earthquake under predominantly similar levels of shaking compared to those in the Sep 2010 earthquake (i.e., within $\pm$ 0.05 *g*). The ground at these sites was likely damaged by the intense Feb 2011 earthquake that produced significant ejecta. This issue is further discussed in Section 5.1.

3.2. Soil profile characteristics

The effect of clean sand deposits and stratified silty soil deposits on the amount of settlement due to ejecta is investigated by showing 102 CPTs at the 44 sites in four groups based on $PGA_{6.1}$ (Fig. 5). These CPTs are within or close to the areas used in the settlement assessment at the 44 sites and are considered to represent the subsurface soil profiles that produced the estimated amounts of ejecta-induced settlement. When a site experienced the $PGA_{6.1}$ within the same range more than once yet had different ejecta-induced settlements, the highest settlement value was used in the analysis. It is important to acknowledge that the number of CPT traces belonging to a different site category is not even within a single $PGA_{6.1}$ bin nor evenly distributed among the four $PGA_{6.1}$ bins. There are more CPTs corresponding to thick, clean sand deposits than highly stratified silty soil deposits. Also, each preceding event within the

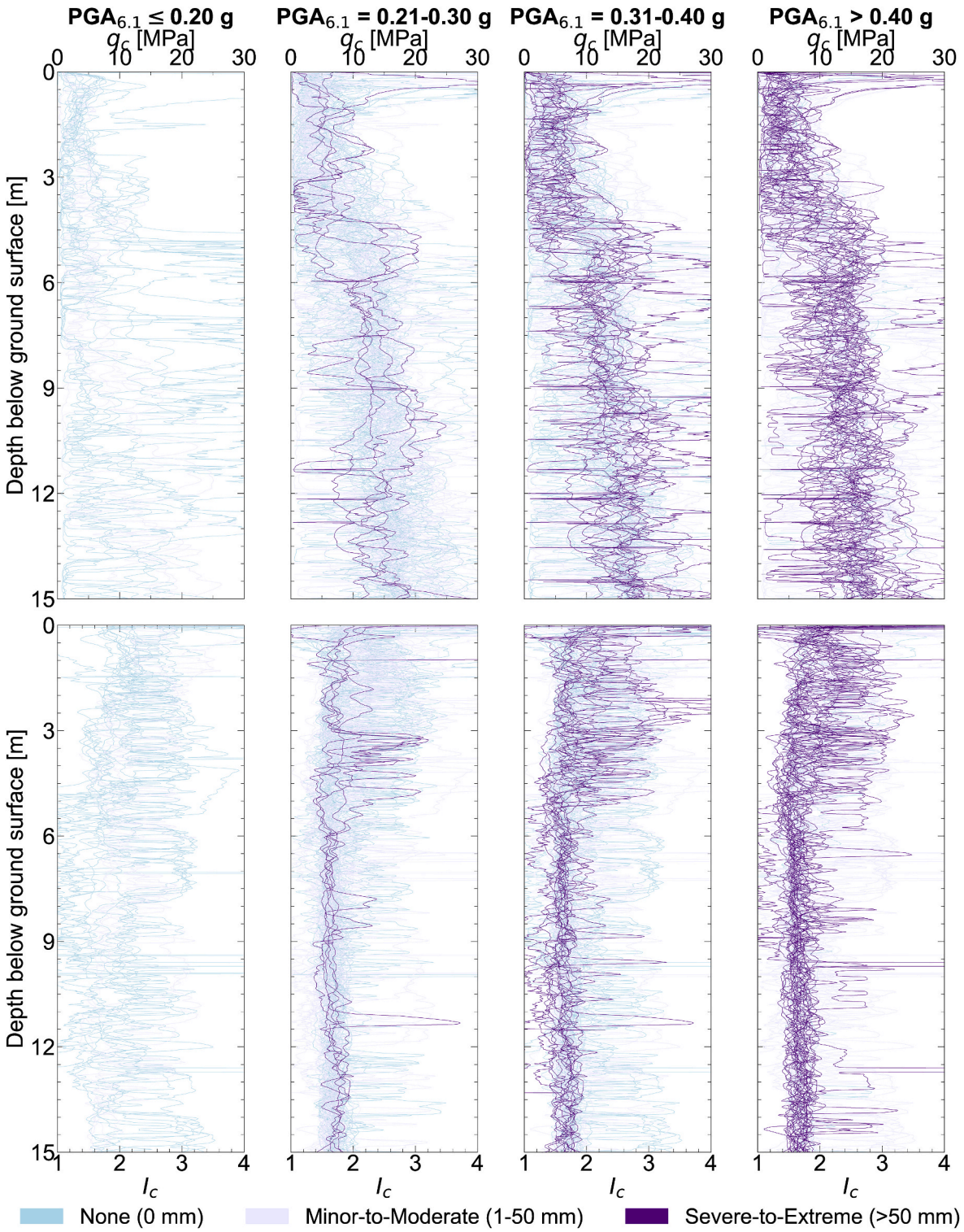

Fig. 5. CPT tip resistance (q_c) and soil behavior type index (I_c) for case histories with none (0 mm), minor-to-moderate (1–50 mm), and severe-to-extreme (> 50 mm) liquefaction ejecta-induced settlement for $PGA_{6.1} \leq 0.20$ *g*, 0.21–0.30 *g*, 0.31–0.40 *g*, and > 0.40 *g*. The CPTs originate from 44 sites that produced ejecta in at least one of the four main Canterbury earthquakes.

Canterbury earthquake sequence could compromise the quality of the crust in a subsequent event and affect the resulting amount of ejecta, as discussed in Section 5.1.

Only none-to-minor ejecta-induced settlement (up to 15 mm) occurs for the $PGA_{6.1} \leq 0.20$ *g* category regardless of the CPT tip resistance (q_c) and I_c of the soil. At higher $PGA_{6.1}$ levels, the severe-to-extreme ejecta-induced settlement is pronounced at sites where $q_c \approx 10$–20 MPa and $I_c \approx 1.3$–1.8 dominate the upper 15 m of the soil profiles, which are typically thick, clean sand deposits. Sites whose soil profiles can be described with $q_c \lesssim 10$–15 MPa and $I_c \approx 2$–3 (i.e., typically stratified silty soil deposits) tend to be more resistant to the formation of ejecta at the ground surface, at least for $PGA_{6.1} \leq 0.40$ *g*. Moreover, sites with severe-to-extreme ejecta-induced settlement typically have silty material in only the top 4–5 m of their soil profiles. Sites with silty material in

at least the top 10 m of the soil profile had none-to-minor ejecta-induced settlement, a trend more obvious for $PGA_{6.1} \leq 0.40$ *g*. $PGA_{6.1}$ = 0.21–0.30 *g* triggered more than 50 mm of ejecta-induced settlement only at soil deposits where sand predominates in the top 15 m of the soil profile.

3.3. Groundwater depth

The effect of groundwater depth on the ejecta-induced settlement for any of the four major Canterbury earthquakes is difficult to discern from regional groundwater depth maps. The groundwater depth at the studied sites ranges from 0.5 m to 3.5 m for all earthquake events. The median groundwater depth for both the Sep 2010 and Feb 2011 case histories datasets is 1.8 m, while the Jun 2011 and Dec 2011 case histories datasets both have a median groundwater depth of 1.5 m. The groundwater depth at a site often varied from earthquake to earthquake. The maximum change in the groundwater depth at a site from earthquake to earthquake ranged from 0 m to 1.0 m with a median of 0.6 m for the 44 sites. Spearman's correlation coefficients for the groundwater depth and the ejecta-induced settlement are weak for the Sep 2010, Jun 2011, and Dec 2011 earthquakes (R_S = −0.27, −0.20, and −0.29, respectively) and very weak for the Feb 2011 earthquake (R_S = −0.03). The coefficients are negative, indicating an increase in the ejecta-induced settlement with a decrease in the groundwater depth.

When the 176 case histories are grouped based on a specified $PGA_{6.1}$ range regardless of the earthquake event, the correlation between the ejecta-induced settlement and the groundwater depth is weak for $PGA_{6.1}$ = 0.21–0.30 *g* (R_S = −0.20) and $PGA_{6.1} > 0.40$ *g* (R_S = −0.31) and very weak for $PGA_{6.1}$ = 0.31–0.40 *g* (R_S = −0.02). When case histories within a specified $PGA_{6.1}$ range are grouped for each individual earthquake, the correlation becomes more significant for the Jun 2011 earthquake with R_S = −0.90 for $PGA_{6.1} > 0.30$ *g*, indicating a decrease in the ejecta-induced settlement with the increasing groundwater depth (Fig. 6b). The negative correlation exists for $PGA_{6.1}$ = 0.21–0.30 *g* too (Fig. 6a); however, it is weak (R_S = −0.25). For the Feb 2011 earthquake and $PGA_{6.1} > 0.30$ *g*, there is a very weak negative correlation between the groundwater depth and the ejecta-induced settlement (R_S = −0.03). The correlation between the Feb 2011 groundwater depth and the settlement becomes positive, and its strength increases to moderate for $PGA_{6.1}$ = 0.31–0.40 *g* (R_S = 0.50). However, if only case histories with $PGA_{6.1} > 0.40$ *g* for the Feb 2011 earthquake are considered, the correlation between the groundwater depth and the ejecta-induced settlement becomes negative, although weak (R_S = −0.32). For the Dec 2011 earthquake, the negative correlation ranges from very weak for $PGA_{6.1}$ = 0.21–0.30 *g* (R_S = −0.18) to moderate for $PGA_{6.1}$ = 0.31–0.40 *g* (R_S = −0.50).

3.4. Crust thickness

Crust thickness can be defined based on I_c and FS_L. In this study, it is the thickness of soil between the ground surface level and the depth at or below the groundwater table where soil has $I_c < 2.6$ or $FS_L < 1$ for at least 200 mm [13]. Hutabarat and Bray [9] used a similar I_c crust thickness definition except they used 250 mm instead of 200 mm as the thickness of a layer at or below the ground water table with $I_c < 2.6$ being defined as the first significant liquefiable layer thickness. This difference has a negligible impact on the observed trends. The FS_L was computed in *CLiq 3.0.3.2* [25] using the Boulanger and Idriss [26] CPT-based liquefaction triggering procedure and the de Greef and Lengkeek [27] thin-layer correction procedure. The thickness is estimated based on the average I_c or FS_L for the CPTs within the most representative settlement assessment area [13].

The crust thickness based on the I_c definition ranges from 0.5 m to 3.6 m for all earthquake events (median = 2.1 m, 2.0 m, 1.7 m, and 1.5 m for the Sep 2010, Feb 2011, Jun 2011, and Dec 2011 events, respectively). Its effect on the ejecta-induced settlement is first analyzed for the four main Canterbury earthquakes altogether and different $PGA_{6.1}$ groups. The $PGA_{6.1} \leq 0.20$ *g* group has only three non-zero ejecta case histories wherein the ejecta-induced settlement values are < 5 mm, < 5 mm, and 15 mm and their respective crust thicknesses are 0.7 m, 2.1 m, and 2.1 m. The $PGA_{6.1}$ = 0.21–0.30 *g* and $PGA_{6.1} > 0.40$ *g* case histories both have a weak tendency toward the higher ejecta-induced settlement with crust thinning (R_S = −0.20 and −0.37, respectively). The ejecta-induced settlement of the $PGA_{6.1}$ = 0.31–0.40 *g* case histories is insignificantly correlated with crust thickness (R_S = 0.02). These observations do not differ much from those for the groundwater depth, which is not surprising considering the incorporation of groundwater depth in the crust thickness definition.

When the effect of crust thickness is analyzed for individual earthquakes and different $PGA_{6.1}$ groups, the results are again like those for the groundwater depth. For $PGA_{6.1} > 0.30$ *g*, the correlation strength between the crust thickness and the ejecta-induced settlement increases to moderate for the Dec 2011 earthquake (R_S = −0.50) and strong for the Jun 2011 earthquake (R_S = −0.78), indicating an increase in the ejecta-induced settlement with the decreasing crust thickness. The Feb 2011 case histories have a positive correlation for $PGA_{6.1}$ = 0.31–0.40 *g* (R_S = 0.38) and a negative correlation for $PGA_{6.1} > 0.40$ *g* (R_S = −0.36); R_S = −0.11 when $PGA_{6.1} > 0.30$ *g*.

It is generally expected that thicker crusts have a beneficial effect in mitigating the surficial manifestation of liquefaction [6]. Obermeier [28] observed a "greatly enhanced" amount of subaerial venting for the meizoseismal region of the 1811–1812 New Madrid earthquakes where the crust was very thin. However, the formation of ejecta through a low-permeability crust on the level ground is driven not only by hydraulic fracturing but also surface ground oscillation cracking, which

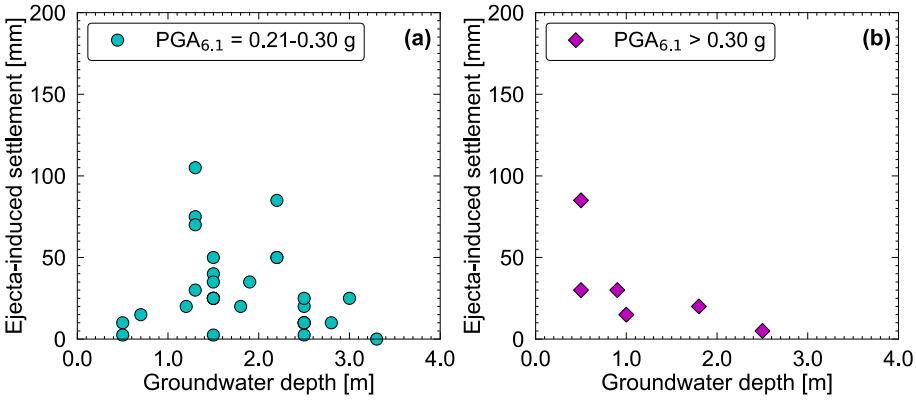

Fig. 6. Ejecta-induced settlement versus groundwater depth for the Jun 2011 earthquake for (a) $PGA_{6.1}$ = 0.21–0.30 *g* (R_S = −0.25) and (b) $PGA_{6.1} > 0.30$ *g* (R_S = −0.90).

can occur independently or in combination with one another [29]. Additionally, venting of liquefied material can be enhanced by holes in the crust such as those left by decayed roots [29,30]. For instance, a sinkhole with ejected material formed in the Feb 2011 earthquake at a location where shrubs had been removed [13]. At this part of the site, the ejecta-induced settlement was extreme compared to the rest of the site with minor ejecta-induced settlement [13].

The ejecta-induced settlement is typically zero when the first liquefiable layer with $FS_L < 1$ (thickness of at least 200 mm) is not within the upper 20 m of the soil profile. For the Sep 2010, Jun 2011, and Dec 2011 earthquakes altogether, 77% of the case histories without the first liquefiable layer being detected have no ejecta-induced settlement. For the Feb 2011 earthquake, the first liquefiable layer is detected in all cases within a 1.0–6.3 m depth range. Extreme ejecta-induced settlements of 120–155 mm are associated with crust thicknesses of 2.1–3.2 m for the Feb 2011 earthquake, and there is a case with no settlement even though the crust is only 1.1 m thick. However, the correlation between ejecta-induced settlement and crust thickness is, among other factors, affected by the reliability of the liquefaction triggering method used to calculate FS_L, which is discussed later.

3.5. First liquefiable layer thickness

The liquefaction ejecta database also contains the thickness of the first significant liquefiable soil layer that may contribute to ejecta production (Z_{ab}) for each case history. The definition originates from the Hutabarat and Bray [9] study wherein a liquefiable soil layer has the following properties: $I_c < 2.6$, is at least 250-mm thick, and extends from the bottom of the crust to the top of a soil layer with $I_c \geq 2.6$ and a minimum thickness of 250 mm. Z_{ab} ranges from 0.5 m to about 14 m for all four main earthquakes with the median Z_{ab} of about 12 m for each earthquake.

For the 176 case histories together, there is a weak tendency for the ejecta-induced settlement to increase with the increasing liquefiable layer thickness ($R_S = 0.27$). The same weak trend exists for the case histories in the $PGA_{6.1} = 0.21$–0.30 *g* and $PGA_{6.1} > 0.40$ *g* groups ($R_S = 0.28$ and 0.39, respectively). The correlation is also positive although very weak for $PGA_{6.1} = 0.31$–0.40 *g* ($R_S = 0.13$). For the Feb 2011 earthquake (Fig. 7), the strength of the positive correlation between the ejecta-induced settlement and Z_{ab} changes from weak for $PGA_{6.1} = 0.31$–0.40 *g* ($R_S = 0.31$) to moderate for $PGA_{6.1} > 0.40$ *g* ($R_S = 0.44$). With all other factors equal, an increase in the ejecta-induced settlement with the increasing thickness of the first liquefiable soil layer is expected.

4. Efficacy of liquefaction-induced damage indices in estimating the severity of ejecta

The efficacy of the Ishihara [8] boundary curves and the liquefaction-induced damage indices (LPI, LSN, and L_D-C_R) in estimating the severity of ejecta-induced settlement is evaluated in the following subsections for all sites in the database, including those that did not produce ejecta in any of the four main Canterbury earthquakes. The true positive rate (TPR), calculated as the number of case histories within a settlement category with the correctly estimated severity of ejecta divided by the total number of case histories within that category, is used to compare the performances of LPI, LSN, and L_D-C_R.

4.1. Ishihara boundary curves

The Ishihara [8] boundary curves provide an opportunity to examine the joint effect of the crust thickness and the liquefiable soil layer thickness on the ejecta-induced settlement for different levels of PGA. The Bradley and Hughes [22,23] PGA estimates for each earthquake event are now scaled using an MSF for an equivalent M_w 7.5 earthquake ($PGA_{7.5}$) for which the curves were developed.

As illustrated in Fig. 8a, the crust thickness for 232 case histories (235 case histories minus three case histories with $PGA_{7.5} = 0.48$ g) does not exceed 5 m, while the thickness of the first liquefiable layer underlying the crust is less than 15 m. Consequently, the data points are clustered in the left third of the plots in Fig. 8. Most data points are located to the left of the 0.20 *g* and 0.45 *g* Ishihara [8] boundary curves, which indicates liquefaction effects should be observed at the ground surface for these cases. However, many of these data points are for the none ejecta-induced settlement category (Fig. 8a), a trend that is most prominent for the Sep 2010 earthquake and least prominent for the Feb 2011 earthquake (Fig. 8b vs. Fig. 8c). The increase in the thickness of the liquefiable soil layer from 1 m to 15 m relative to the typical 1–4 m range of the overlying crust thickness does not have a notable effect on the ejecta-induced settlement for the Sep 2010 earthquake regardless of $PGA_{7.5}$. Conversely, most none ejecta-induced settlement points for the Feb 2011 earthquake (79%, Fig. 8c–ii) are for the liquefiable layer thickness less than 1.2 m. It is difficult to evaluate the importance of the thickness of the crust with the Mijic et al. [13] data because there are few cases when the crust thickness is greater than 3 m.

4.2. Liquefaction potential index

The ejecta-induced settlement is compared with LPI [5], which is defined as:

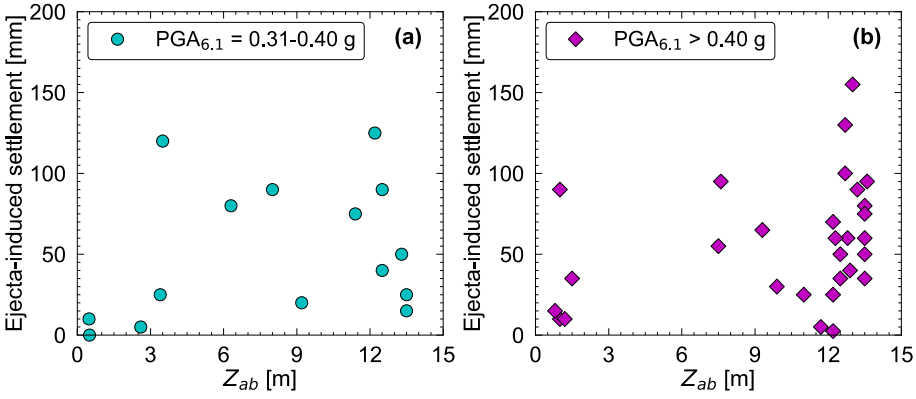

Fig. 7. Ejecta-induced settlement versus first significant liquefiable layer thickness (Z_{ab}) for the Feb 2011 earthquake for (a) $PGA_{6.1} = 0.31$–0.40 *g* ($R_S = 0.31$) and (b) $PGA_{6.1} > 0.40$ *g* ($R_S = 0.44$).

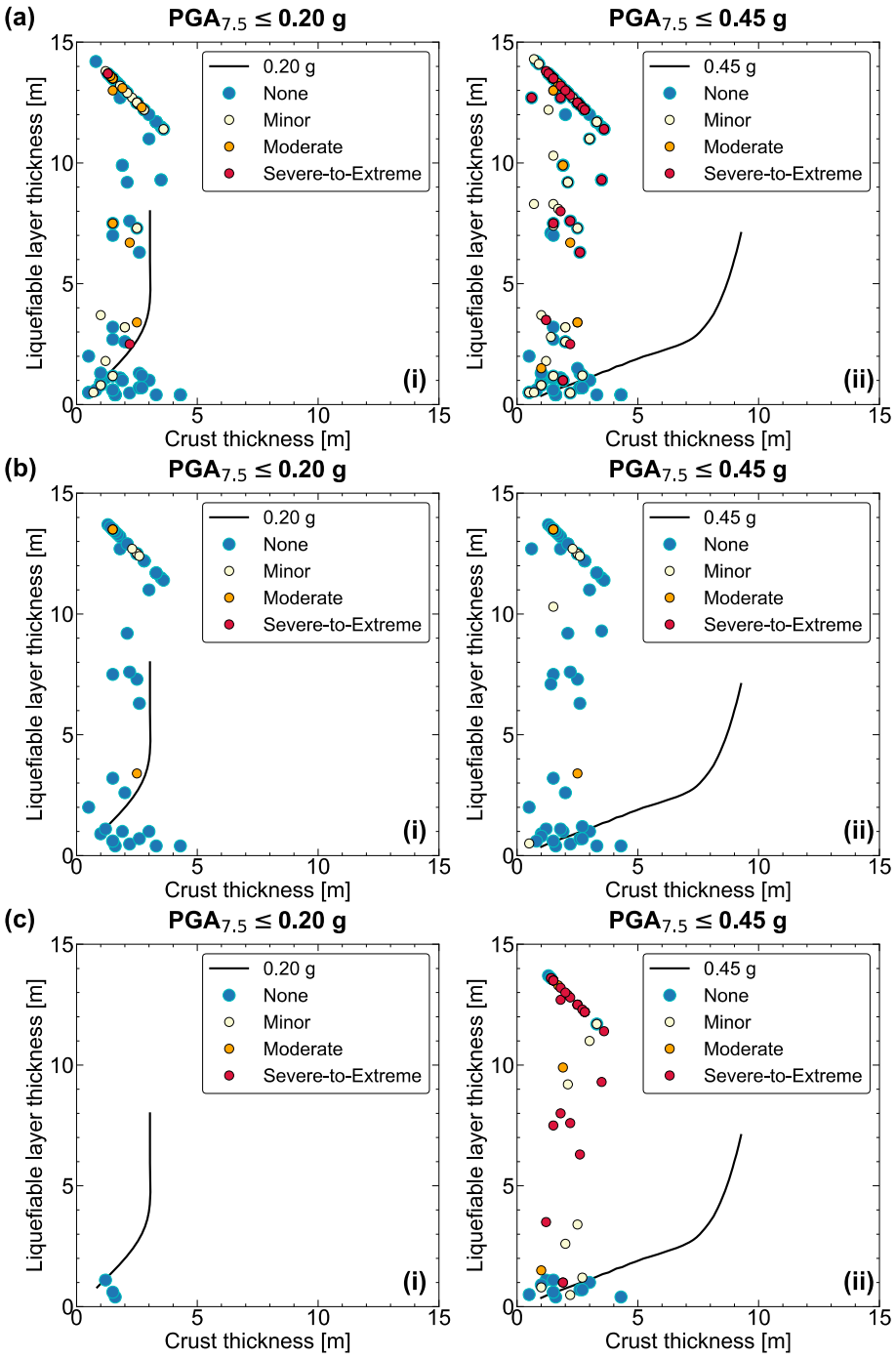

Fig. 8. None (0 mm), minor (1–25 mm), moderate (26–50 mm), and severe-to-extreme (>50 mm) liquefaction ejecta-induced settlement for (a) all four main Canterbury earthquakes, (b) Sep 2010 earthquake, and (c) Feb 2011 earthquake for (i) $PGA_{7.5} \leq 0.20\ g$ and (ii) $PGA_{7.5} \leq 0.45\ g$ relative to the Ishihara [8] boundary curves. The crust and liquefiable layer thicknesses are defined per Hutabarat and Bray [9].

$$LPI = \int_{0\ m}^{20\ m} F\ w(z)dz$$

where $F = 1 - FS_L$ for $FS_L \leq 1$ and $F = 0$ for $FS_L > 1$, $w(z) = 10 - 0.5z$, and z is the depth in meters below the ground surface. LPI assumes the severity of liquefaction manifestation is proportional to the liquefiable layer thickness and its proximity to the ground surface and the amount by which FS_L is less than 1. LPI is sensitive to groundwater depth at sites with shallow saturated, liquefiable layers. The criterion for LPI and the observed liquefaction ejecta-induced settlement used in this study is based on the study by Maurer et al. [31]. The liquefaction ejecta-induced settlement is estimated as none, minor, moderate, and severe-to-extreme if LPI = 0–4, 4–8, 8–15, and ≥ 15, respectively.

LPI correctly estimates the absence of ejecta in 89% of case histories corresponding to thick, clean sand sites and 69% of case histories corresponding to stratified silty sites (Table 2). As the ejecta-induced settlement at thick, clean sand sites increases, LPI tends to increasingly underestimate its severity at the Christchurch sites (Fig. 9a–i). It underestimates the ejecta-induced settlement for 67%, 58%, and 86% of case histories with minor, moderate, and severe-to-extreme ejecta-induced settlement, respectively. The median LPI values for minor,

Table 2
True positive rate (TPR) of LPI, LSN, and L_D-C_R for 165 case histories represented by thick, clean sand sites and 60 case histories represented by stratified silty soil sites.

Ejecta-induced settlement category	TPR [%]					
	Thick, clean sand sites			Stratified silty soil sites		
	LPI	LSN	L_D-C_R	LPI	LSN	L_D-C_R
None (0 mm)	89 (N = 70)	81	77	69 (N = 45)	56	91
Minor (1–25 mm)	29 (N = 48)	40	17	0 (N = 13)	8	8
Moderate (26–50 mm)	26 (N = 19)	16	26	0 (N = 1)	0	0
Severe-Extreme (> 50 mm)	14 (N = 28)	18	64	100 (N = 1)	0	100

Notes: N = number of case histories; TPR = true positive rate (i.e., percentage of case histories with correctly estimated ejecta-induced settlement relative to the total number of case histories within the specified settlement category); Stratified silty sites include both highly and partially stratified silty sites.

moderate, and severe-to-extreme ejecta-induced settlement categories at thick, clean sand sites are 1, 3, and 6, respectively, which are well below the respective lower boundaries of 4, 8, and 15. Conversely, LPI tends to overestimate the ejecta-induced settlement at stratified silty sites (Fig. 9a–ii). The median LPI for the minor ejecta-induced settlement category is 12 compared to the upper boundary of 8. LPI overestimates the minor ejecta-induced settlement in 62% of case histories corresponding to stratified silty soil sites. Moreover, the underestimation of non-zero ejecta-induced settlement at thick, clean sand sites is present for each of the four main earthquakes, whereas the overestimation of zero ejecta-induced settlement at stratified silty soil sites is absent for the Jun 2011 and Dec 2011 earthquakes compared to the Sep 2010 and Feb 2011 earthquakes (the overestimation occurs for 57% and 75% of no-ejecta case histories, respectively). The systematic underestimation or overestimation of ejecta severity by liquefaction-induced damage indices, such as LPI, is primarily due to the absence of incorporation of system-response effects in simplified liquefaction assessment procedures [10,11,17,32].

4.3. Liquefaction severity number

The ejecta-induced settlement is also compared with LSN [6], which is defined as:

$$LSN = 1,000 \int \frac{\varepsilon_v}{z} dz$$

where ε_v is the post-liquefaction volumetric strain provided as a decimal and z is the depth in meters below the ground surface ($z > 0$ m). The ejecta-induced settlement is estimated as none, minor, moderate, severe, and extreme if LSN = 0–10, 10–20, 20–30, 30–40, and ≥ 40, respectively, based on Hutabarat and Bray [9]. For comparison with LPI, the severe and extreme categories are combined into a single severe-to-extreme category if LSN ≥ 30.

The TPR indicates the overall performance of LSN in terms of estimating the ejecta-induced settlement correctly does not differ much from that of LPI (Table 2). The TPR of LSN for the no-ejecta case histories is slightly lower than that of LPI at both thick, clean sand sites and stratified silty sites by 8% and 13%, respectively. The TPR of LSN for severe-to-extreme ejecta at thick, clean sand sites is higher than that of LPI by 4%. Moreover, the underestimation of ejecta-induced settlement at thick, clean sand sites by LSN is prominent for all non-zero ejecta-induced settlement categories (Fig. 9b–i). The median LSN values corresponding to minor, moderate, and severe-to-extreme ejecta-induced settlement categories at thick, clean sand sites are 8, 14, and 15, respectively, compared to the respective lower boundaries of 10, 20, and 30. At stratified silty soil sites, like LPI, LSN tends to overestimate the ejecta-induced settlement (Fig. 9b–ii). LSN also overestimates the severity of ejecta-induced settlement in 62% of case histories with minor ejecta at stratified silty sites. The median LSN for minor ejecta-induced settlement at stratified silty sites is 25 compared to the upper boundary of 20. Further, LSN underestimates the non-zero ejecta-induced settlement at thick, clean sand sites for each of the four main earthquakes. Overestimation of zero ejecta-induced settlement at stratified silty sites by LSN is greater for the Sep 2010 and Feb 2011 earthquakes (79% and 88% for the no-ejecta cases, respectively) than for the Jun 2011 and Dec 2011 earthquakes (20% and 0% for the no-ejecta cases, respectively).

4.4. Liquefaction ejecta demand and crust resistance parameters

The ejecta-induced settlement is compared with L_D and C_R, which are defined by Hutabarat and Bray [9] in their CPT-based procedure as:

$$L_D\left(\frac{kN}{m}\right) = \gamma_w \int_{z_a}^{z_b} \frac{k_v}{k_{cs}}(h_e - h_c)dz \begin{cases} when \quad h_e \geq h_c \\ 0, \ otherwise \end{cases}$$

$$C_R\left(\frac{kN}{m}\right) = \int_0^{z_a} s_u dz \begin{cases} s_u = K_o \sigma'_{vo} tan\left(\varphi_{cs}\right), \ if \ I_B > 22 \ (sand-like \ soil) \\ s_u = \frac{q_t - \sigma_{vo}}{N_{kt}}, \ if \ I_B \leq 22 \ (clay-like \ soil) \end{cases}$$

where z_a is the depth from the ground surface to the top of the first liquefiable soil layer (i.e., the first soil layer below the groundwater table with $I_c < 2.6$ and at least 250-mm thick), z_b is the depth from the ground surface to the top of the first non-liquefiable soil layer underlying the previously defined liquefiable layer (i.e., it is a depth to the first soil layer located between z_a and 15-m depth with $I_c \geq 2.6$ and thickness ≥ 250 mm), k_v is the vertical hydraulic conductivity, k_{cs} is the hydraulic conductivity of clean sand, h_e is the excess hydraulic head, h_c is the required h_e at a depth z to produce significant ejecta, s_u is the shear strength of crust with $N_{kt} = 15$ for clayey soil, and $K_o = 0.5$ and $\varphi_{cs} = 33°$ for sandy soil. The Hutabarat and Bray [9] liquefaction ejecta severity chart has none-to-minor, minor-to-moderate, and moderate-to-severe-extreme zones separated by bilinear boundaries defined by three [C_R, L_D] data points in kN/m: [0, 2.5], [100, 2.5], and [250, 25]; [0, 6], [90, 6], and [250, 70]; and [0, 15], [85, 15], and [250, 150], respectively.

The relationships between the ejecta-induced settlement and C_R and L_D are first examined for 176 case histories corresponding to the sites that had ejecta in at least one of the four main Canterbury earthquakes. There is a general tendency for the ejecta-induced settlement to decrease with the increasing C_R. For example, there are no cases with $PGA_{6.1} \leq 0.30$ *g* with more than 30 mm of ejecta-induced settlement when C_R is greater than 45 kN/m. Spearman's correlation coefficient of −0.40 for the case histories with $PGA_{6.1} > 0.40$ *g* also supports this trend. $R_S = -0.21$ (weak) for $PGA_{6.1} = 0.21$–0.30 *g* and $R_S = 0.12$ (very weak) for $PGA_{6.1} = 0.31$–0.40 *g*. Furthermore, the L_D values for the less damaging Sep 2010, Jun 2011, and Dec 2011 earthquakes do not exceed 41, 38, and 62 kN/m, respectively, while the maximum L_D for the Feb 2011 earthquake that produced the most ejecta is 164 kN/m. There is a weak tendency for the ejecta-induced settlement to increase with an increase in L_D, as indicated by R_S of 0.24 for the Feb 2011 earthquake, and a moderate tendency toward the same trend for the Jun 2011 and Dec 2011 earthquakes ($R_S = 0.43$ and 0.44, respectively). When the correlation is analyzed for all 176 data points (i.e., for the four main Canterbury earthquakes together), $R_S = 0.59$, which indicates a moderate positive correlation between ejecta-induced settlement and L_D.

Considering again all thick, clean sand sites and stratified silty sites, including those that did not produce ejecta in any of the four main Canterbury earthquakes, the TPR of the Hutabarat and Bray [9] L_D-C_R chart for zero ejecta-induced settlement at stratified silty sites is 91%

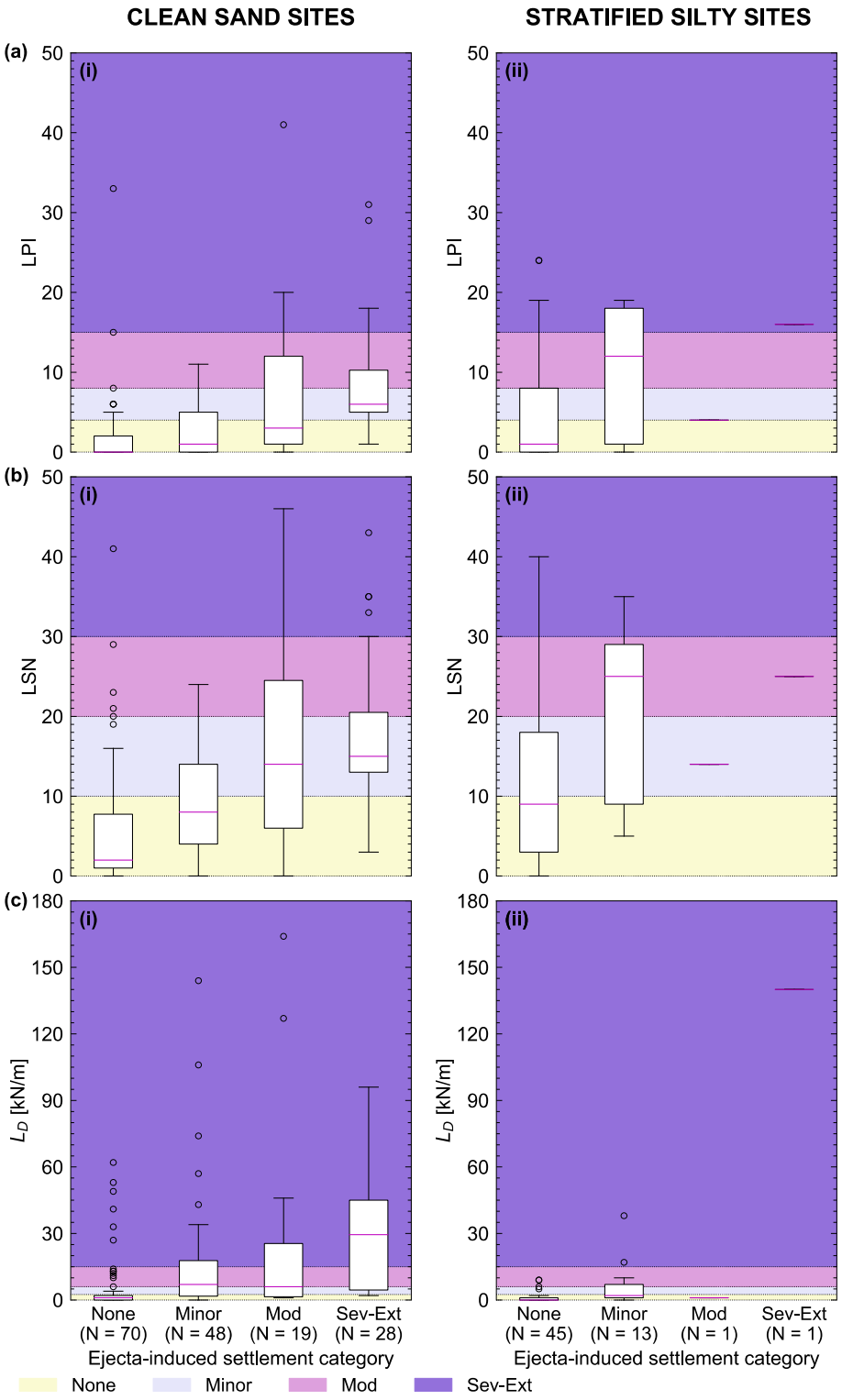

Fig. 9. Performance of (a) liquefaction potential index, LPI, (b) liquefaction severity number, LSN, and (c) liquefaction ejecta demand, L_D, for case histories corresponding to (i) clean sand sites and (ii) stratified silty soil sites relative to the none, minor, moderate, and severe-to-extreme ejecta-induced settlement categories.

compared to TPR = 69% and 56% of LPI and LSN, respectively (Table 2). By comparison, the efficacy of the L_D-C_R chart in correctly estimating the zero ejecta-induced settlement at thick, clean sand sites is slightly lower than the efficacies of LPI and LSN (TPR = 77% compared to 89% and 81%, respectively). The L_D-C_R chart outperforms both LPI and LSN in the case of severe-to-extreme ejecta-induced settlement at thick, clean sand sites (TPR = 64% compared to 14% and 18%, respectively). The median L_D for the severe-to-extreme ejecta-induced settlement category is 30 kN/m, which is well above the boundary of 15 kN/m (Fig. 9c-i). Further, the misestimation of zero and non-zero ejecta-induced settlement at thick, clean sand sites by the L_D-C_R chart occurs for all earthquake events, whereas the overestimation of zero ejecta-induced settlement at stratified silty soil sites by the L_D-C_R chart does not occur for the Jun 2011 and Dec 2011 case histories. Overestimation of zero settlement at

stratified silty sites occurs for 7% and 38% of the Sep 2010 and Feb 2011 no-ejecta cases, respectively. Finally, L_D does not distinguish well between minor and moderate ejecta-induced settlement at thick, clean sand sites (Fig. 9c–i). The respective median L_D values are 7 kN/m and 6 kN/m compared to L_D = 6 kN/m that divides the two categories. At stratified silty sites, the median L_D for minor ejecta-induced settlement is 2 kN/m, which is below the lower boundary of 2.5 kN/m (Fig. 9c–ii).

4.5. Summary

In reviewing Table 2, the primary advantage of the L_D-C_R chart relative to LPI and LSN is its ability to identify stratified silty soil sites where no ejecta-induced settlement is likely to occur at a TPR of 91%. The L_D-C_R chart resolves the overestimation of liquefaction-induced ground failure and ejecta-induced settlement at stratified silty soil sites by simplified liquefaction triggering procedures and liquefaction-induced ground damage indices, such as LPI and LSN, that rely on FS_L from these procedures. LPI is slightly better than LSN and the L_D-C_R chart in identifying thick, clean sand sites with no ejecta. All these parameters struggle to achieve high TPR values in identifying sites with minor or moderate levels of ejecta-induced settlement for the cases investigated in this study. Lastly, the L_D-C_R chart is the most successful identifier of sites with severe-to-extreme ejecta-induced settlement. Thus, with the L_D-C_R chart, an engineer can most confidently identify sites where the ejecta-induced settlement will be none or where it will be significant (i.e., > 50 mm). Additional ejecta-induced settlement field case histories should be interrogated when they become available.

5. Site conditions conducive to the formation or abatement of ejecta

5.1. Earthquake sequence and site performance differences

The examination of the 58 sites in the liquefaction ejecta database for all four main earthquakes reveals that ejecta were not generated by the Jun 2011 earthquake or Dec 2011 earthquake if the Feb 2011 earthquake did not result in the formation of ejecta. There are 14 sites that never generated ejecta during the Canterbury earthquake sequence. The most common earthquake combination in the database that generated ejecta-induced settlement includes the Feb 2011 and Jun 2011 earthquakes (32 sites). These 32 sites are predominantly thick, clean sand sites (28 of 32 sites). The sites typically experienced $PGA_{6.1}$ levels that were only slightly higher in the Jun 2011 earthquake than in the Sep 2010 earthquake (Fig. 10a). The median $PGA_{6.1}$ values for the 32 sites are 0.23 *g* and 0.25 *g* for the Sep 2010 and Jun 2011 earthquakes, respectively. The groundwater depth was generally only slightly shallower during the Jun 2011 earthquake than the Sep 2010 earthquake (Fig. 10b). The median groundwater depths for the 32 sites are 1.8 m and 1.5 m for the Sep 2010 and Jun 2011 earthquakes, respectively. The median values of these sites' first liquefiable layer thicknesses are similar for the Sep 2010 and Jun 2011 earthquakes (12.2 m and 12.4 m, respectively), as shown in Fig. 10c. The crust thickness is slightly greater for the Sep 2010 earthquake than the Jun 2011 earthquake (Fig. 10d) with median crust thicknesses of 2.1 m and 1.6 m for the respective earthquakes. The scatter in the data is like that in Fig. 10b, which is not surprising considering the utilization of groundwater depth in the crust thickness definition.

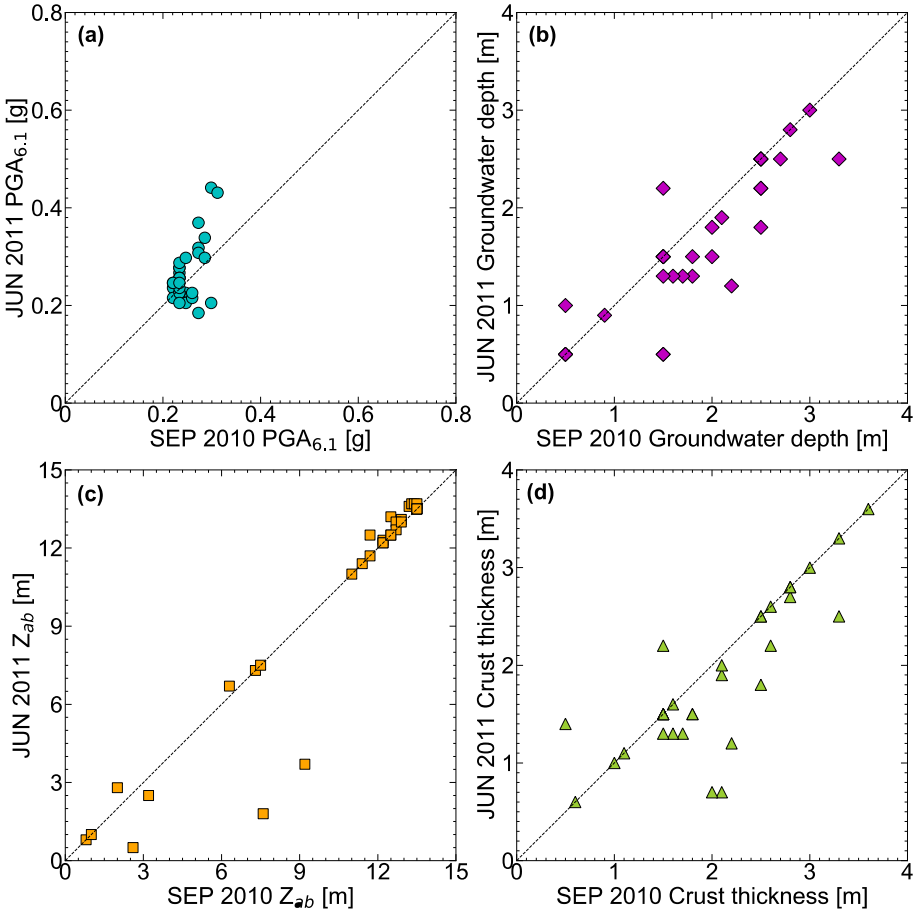

Fig. 10. Comparison of (a) $PGA_{6.1}$, (b) groundwater depth, (c) first liquefiable soil layer thickness, and (d) crust thickness for the Sep 2010 and Jun 2011 earthquakes at sites that did not manifest ejecta in the Sep 2010 earthquake but manifested it in the Jun 2011 earthquake.

All 32 sites without ejecta in the Sep 2010 earthquake but with ejecta in the Jun 2011 earthquake were strongly shaken during the Feb 2011 earthquake ($PGA_{6.1} \geq 0.35$ *g*) and underwent at least 5 mm of ejecta-induced settlement. Fig. 11 shows the ejecta-induced settlement for the Jun 2011 earthquake tends to increase with increasing ejecta-induced settlement for the Feb 2011 earthquake. Spearman's correlation coefficient of 0.73 confirms this trend is strong. Additionally, compared to the $PGA_{6.1}$ levels that produced ejecta at the 32 sites in the Feb 2011 earthquake (median $PGA_{6.1} = 0.44$ *g*), lower $PGA_{6.1}$ levels were sufficient to trigger the formation of ejecta at the same sites in the Jun 2011 earthquake (median $PGA_{6.1} = 0.25$ *g*). All the above implies that extensive liquefaction ejecta in the Feb 2011 earthquake severely damaged the land and formed cracks through which the liquefied soil migrated more easily to the ground surface during the Jun 2011 earthquake. Recurrence of liquefaction ejecta at the same site and via the same path through the crust is not uncommon [29].

The sites did not manifest ejecta in the Dec 2011 earthquake if they did not manifest ejecta in the Jun 2011 earthquake (apart from one site with the ejecta-induced settlement of < 5 mm). However, only 63% (20/32) of the sites with ejecta in the Feb 2011 and Jun 2011 earthquakes manifested ejecta in the Dec 2011 earthquake too. Sites that did not have ejecta in Dec 2011 were shaken with $PGA_{6.1}$ that was similar to (within $\pm$ 0.05 *g*) or lower than that in Jun 2011, while sites with ejecta in Dec 2011 experienced $PGA_{6.1}$ that was similar to (within $\pm$ 0.05 *g*) or higher than that in Jun 2011. At most sites (85%, 17/20), the Dec 2011 ejecta-induced settlement did not exceed 30 mm. Three sites underwent severe-to-extreme ejecta-induced settlement in Dec 2011 (65–120 mm). These three sites also had severe-to-extreme ejecta-induced settlement in the Jun 2011 earthquake (70–105 mm) unlike 88% (15/17) of the sites that had minor-to-moderate (up to 50 mm) ejecta-induced settlement in Jun 2011. The other 12% of the sites experienced severe Jun 2011 ejecta-induced settlement (75–85 mm) but minor Dec 2011 ejecta-induced settlement (5–15 mm). Fig. 12 illustrates a moderate tendency for an increase in the Dec 2011 ejecta-induced settlement with an increase in the Jun 2011 ejecta-induced settlement ($R_S = 0.47$). Additionally, sites with $PGA_{6.1} \leq 0.30$ *g* in Dec 2011 did not produce more than 10 mm of ejecta-induced settlement regardless of the amount of settlement in the Jun 2011 earthquake.

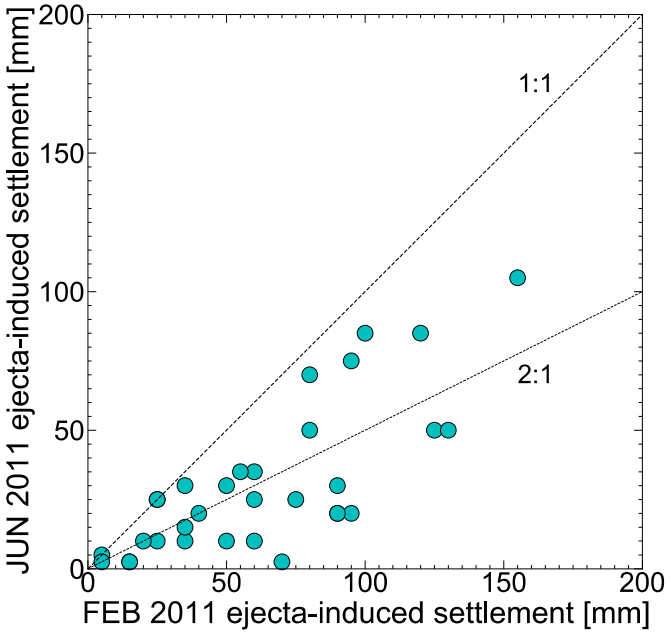

Fig. 11. The ejecta-induced settlement for the Jun 2011 earthquake relative to the ejecta-induced settlement for the Feb 2011 earthquake. ($R_S = 0.73$)

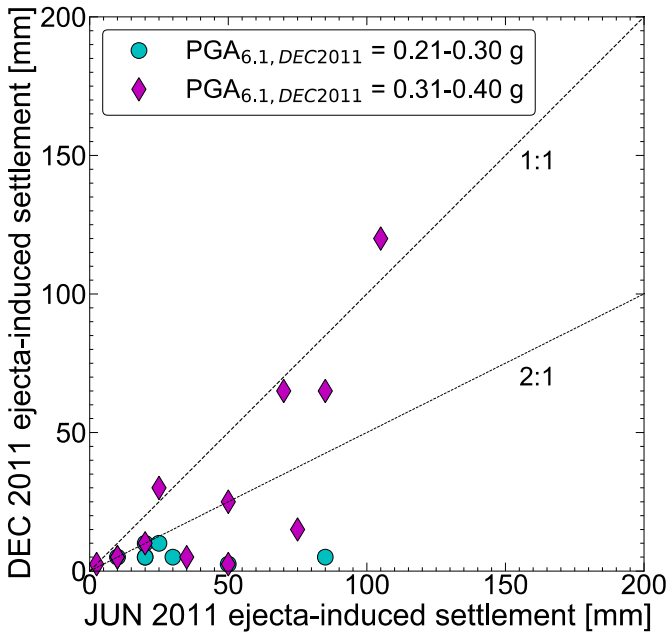

Fig. 12. The ejecta-induced settlement for the Dec 2011 earthquake relative to the ejecta-induced settlement for the Jun 2011 earthquake at 20 sites that manifested ejecta in the Feb 2011 earthquake too. ($R_S = 0.47$)

5.2. Distribution of ejecta at sites with elevated ground

The severity of ejecta tended to be lower at residential properties that were at higher elevations relative to the adjacent roads that had ejecta (Table S1 in supplementary material). Twenty sites with considerable elevation differences between residential properties and roads were identified using the LiDAR-based digital elevation model (DEM). The elevation difference between properties and roads was either constant along an entire road length or it ranged from 0 m to 2 m at most. The median of the average elevation difference at these sites was 0.5 m. Based on the high-resolution aerial photograph for the Feb 2011 earthquake and property inspection reports, ejecta were primarily on the road for 65% (13/20) of the sites and it tended to increase in areal coverage with an increasing elevation difference. No difference in the distribution of ejecta across properties and roads was discernible for 30% (6/20) of the sites, of which one-third had noticeably more ejecta at properties with a lower ground surface elevation within the site. Only one of the 20 sites had ejecta mostly on properties that occupied parts of the site with the lowest elevation. Interestingly, the LiDAR-based difference DEM for the Feb 2011 earthquake often showed more liquefaction-induced settlement (due mostly to post-liquefaction reconsolidation) occurred at parts of sites with higher elevations and less ejecta. The database also contains 11 sites (with a significant portion of the road within the 50-m buffer) with ejecta in the Feb 2011 earthquake but without observable elevation differences between properties and adjacent roads. Ejecta were present on both properties and roads at nearly all sites and were typically distributed similarly across them. Only one site had ejecta exclusively on the residential properties.

The performance differences in the Feb 2011 earthquake between residential properties and adjacent roads at two sites with a discernible elevation difference between the properties and the adjacent roads are displayed in Fig. 13. CPTs indicate the property and road subsurface soil profiles do not differ much at these sites that contain more than 3 m of clean saturated sand. The Sandown Cres site has a 0.5–1 m elevation difference between the properties and the road. The greatest elevation difference of 1 m occurs between the properties in the southeast quadrant of the site and the road. Similarly, the amount of ejecta at this section of the road is greater than that in the northwest quadrant with

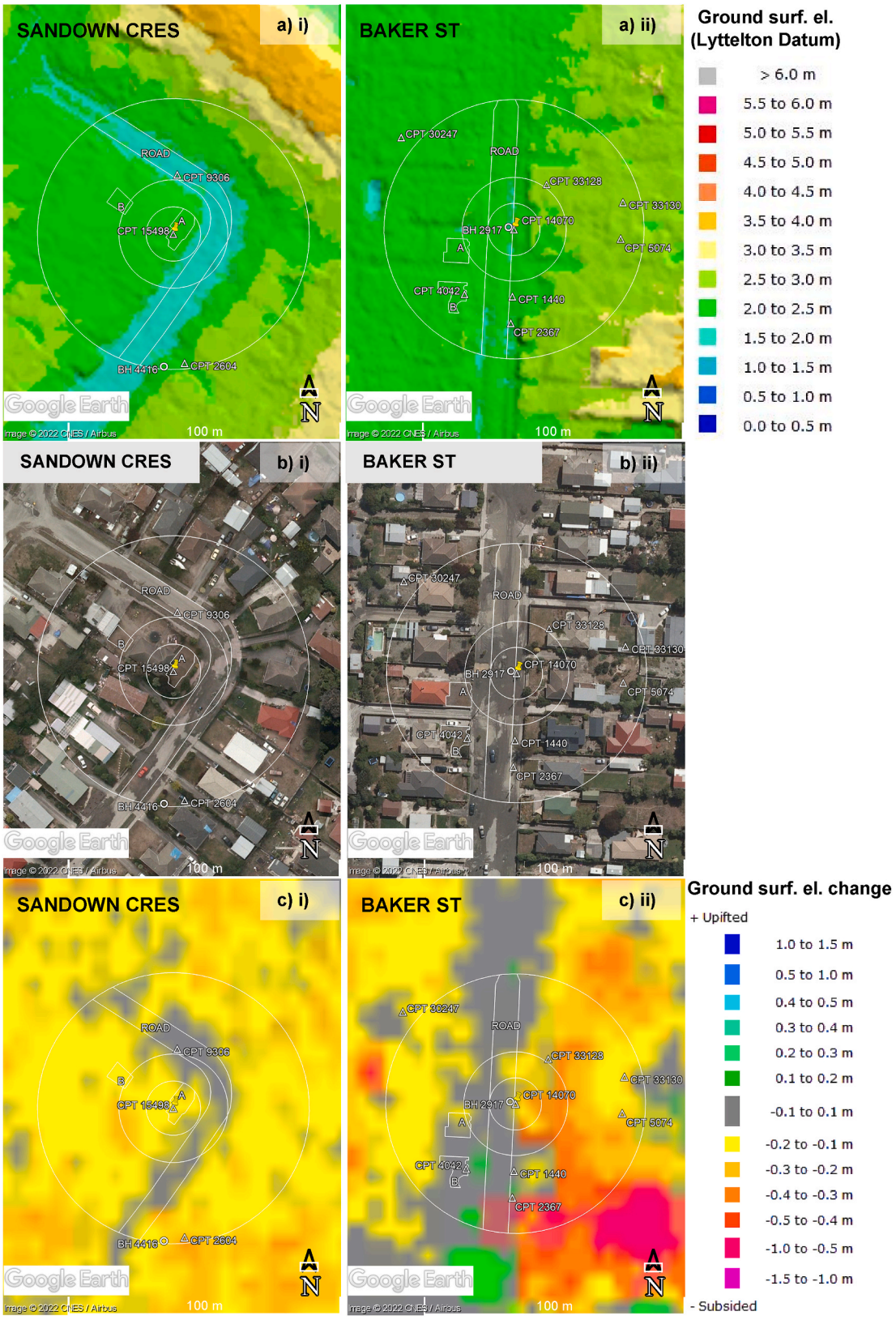

Fig. 13. (a) Sep 2011 ground surface elevation [33], (b) Feb 2011 aerial photograph [34], and (c) Feb 2011 liquefaction-induced settlement [35] for the (i) Sandown Cres and (ii) Baker St sites. The ground surface elevation and settlement models are based on LiDAR data. White circles indicate the 10-, 20-, and 50-m radial areas around the center of the site.

the lowest elevation difference. The ejecta-induced settlement at the properties ranges from 0 mm (Patch A) to 35 ± 55 mm (Patch B). The ejecta-induced settlement of the portion of the road within the 20-m buffer is 85 ± 10 mm, while the ejecta-induced settlement of the entire road (i.e., within the 50-m buffer) is 50 ± 10 mm. The Baker St site also has significantly more ejecta on the road compared to the surrounding properties. The elevation difference of 0.5–1 m exists between the properties in the eastern half of the site and the road. The properties in the western half of the site are at a ground surface elevation similar to that of the road and generally have more ejecta than the properties in the eastern half of the site with the greater ground surface elevation. The ejecta-induced settlement at the properties ranges from 0 mm to 40 ± 10 mm, whereas the ejecta-induced settlement of the entire road (i.e., within the 50-m buffer) is 145 ± 30 mm. The LiDAR-based difference DEM indicates the elevated properties at both sites settled substantially more than the roads because of liquefaction.

The origin of the ejecta on the road cannot be discerned unequivocally. It is most likely the liquefied soil was expelled through drains or cracks on the road, but it could have also been transported by lateral flow from the adjacent residential properties. The roads initially have thin, relatively impermeable crusts with an underlying layer of sand, gravel, or crushed stone, which would restrict upward flow of liquefied soil. However, cracks that form in the pavement as well as crust defects near the road (e.g., holes for light poles, buried pipes, and storm drains) provide a preferential path for liquefied soil to migrate up through to form ejecta on the road surface. The elevated residential properties have a thicker crust comprised of low-permeability topsoil, which overlies the native soil deposit. Thus, liquefied soil could have also flowed laterally toward the defects and thinner crust adjacent to the road.

5.3. Sites without ejecta in the Canterbury earthquake sequence

The 14 sites that did not produce ejecta in the Canterbury earthquakes (Table 3) are characterized by highly stratified silty soil deposits (4 sites), partially stratified silty soil deposits (4 sites), and thick, clean sand deposits (6 sites). All sites experienced similar $PGA_{6.1}$ in the Sep 2010 earthquake (median = 0.28 *g*). The thick, clean sand sites experienced generally higher $PGA_{6.1}$ than the stratified silty soil sites in the earthquakes of Feb 2011 (median = 0.56 *g* vs. 0.34 *g*), Jun 2011 (median = 0.26 *g* vs. 0.18 *g*), and Dec 2011 (median = 0.29 *g* vs. 0.16 *g*). However, the stratified silty sites had shallower groundwater depths in the main Canterbury earthquakes compared to the thick, clean sand sites (median = 1.5 m vs. 2.4 m). Similarly, the median crust thickness at the stratified silty sites in the main Canterbury earthquakes was lower than that at the thick, clean sand sites (1.5 m vs. 2.4 m). The following two sections discuss the absence of ejecta at stratified silty sites and thick, clean sand sites with a focus on the Feb 2011 earthquake because it caused the most severe shaking at these sites (except at the 70 Langdons St and Marblewood Reserve sites that experienced slightly stronger shaking in the Sep 2010 earthquake, $PGA_{6.1}$ = 0.27 *g* and 0.29 *g*, respectively, but still did not manifest ejecta).

5.3.1. Stratified silty sites

Four highly stratified and four partially stratified silty soil sites had no ejecta-induced settlement in the main Canterbury earthquakes (Table 3 and Fig. 14, and Figs. S1 and S2 in supplementary material). They are situated in the SW or NW quadrants, apart from the Kensington St which is in the NE quadrant. Each stratified silty soil deposit represents a system of multiple soil layers of contrasting permeabilities and liquefaction susceptibilities, which has the potential to abate the manifestation of liquefaction at ground surface [10,17].

The severity of liquefaction-induced damage at six of these stratified silty sites is significantly overestimated by LSN and LPI (Table 3). The damage is correctly estimated by LSN and LPI at the Kensington Ave site only and is only slightly overestimated by LSN at the 70 Langdons St site. The 70 Langdons St site experienced a relatively low $PGA_{6.1}$ in the Feb 2011 earthquake (0.24 *g*). It is highly stratified with a 4.9-m thick layer of non-liquefiable clayey soil at a 4.5-m depth and only three thin, clean sand layers (0.3–0.7 m in thickness). The Kensington Ave site is partially stratified with a 3.8-m thick layer of non-liquefiable soil at a depth of 2.1 m (Fig. 14a). The $PGA_{6.1}$ at this site is comparable to that at the St. Teresa School site for which the ejecta-induced damage is significantly overestimated by LSN and LPI (Table 3). The St. Teresa School site has more soil layers with cyclic resistance ratio (CRR) lower than CSR throughout the 15-m deep profile (Fig. 14b). It has only several thin layers of clean sand with an average corrected tip resistance (q_t) of 6–9 MPa between silty and clayey soil layers, whereas the Kensington Ave site has three clean sand layers in a depth range from 6.8 m to 15 m with a total thickness of 7.7 m, an average q_t ranging from about 12 MPa to 20 MPa, and CRR > CSR.

The L_D-C_R chart correctly estimates the ejecta-induced damage at all highly stratified silty sites and overestimates it at partially stratified silty sites – significantly at Wharenui School and Kensington Ave and slightly at St. Teresa's School and 200 Cashmere Rd. The Wharenui School and 200 Cashmere Rd sites are similar to the St. Teresa School site in that they have more thin layers of contrasting permeabilities and thinner layers of clean sand than the Kensington Ave site. The Wharenui School site has the deepest groundwater table among all silty sites (Table 3) and a layer of gravel that extends from a depth of 11 m to a depth of at least 15 m based on the CPT and borehole log. The 200 Cashmere Rd site has a

Table 3
The ground motion and site characteristics for the Feb 2011 earthquake for 14 sites without ejecta in the Canterbury earthquakes.

Site name		$PGA_{6.1}$ [g]	GWT [m]	$*Z_a$ [m]	$*FS_L < 1$ crust thickness [m]	$*Z_{ab}$ [m]	*LSN	*LPI	$*L_D$ [kN/m]	$*C_R$ [kN/m]
Highly stratified silty soil sites	70 Langdons Rd	0.24	1.5	1.6	3.5	0.4	11	3	0	26
	Gainsborough Res	0.44	1.5	2.7	2.7	0.7	28	24	1	27
	455 Papanui Rd	0.28	1.2	1.2	2.4	0.7	17	7	0	4
	Marblewood Res	0.25	1.5	1.5	3.7	0.6	18	7	1	6
Partially stratified silty soil sites	St. Teresa's School	0.35	0.9	1.0	1.5	0.9	38	24	3	23
	Wharenui School	0.37	2.3	3.2	2.3	0.9	14	8	17	30
	200 Cashmere Rd	0.47	1.0	1.0	1.1	0.5	20	13	4	4
	Kensington Ave	0.33	1.5	1.5	6.0	0.6	8	3	9	10
Thick, clean sand sites	Rawhiti Domain	0.54	1.3	1.3	18	13.7	1	0	1	5
	Palinurus Rd 1	0.70	1.3	1.5	1.5	5.5	37	30	12	23
	Keers Rd	0.65	1.2	1.4	8.1	13.6	2	1	4	19
	Armagh St	0.47	3.5	4.6	4.6	0.4	9	6	3	61
	Lakewood Dr	0.35	3.0	3.0	4.3	1.0	8	3	0	23
	Tonks St	0.57	3.3	3.3	8.5	11.7	1	1	7	33

Notes: *Based on a CPT at the center of each site, apart from a CPT at the Palinurus Rd 1 site that is 10 m away from the center; GWT = groundwater table; Z_a = crust thickness per Hutabarat and Bray [9] definition; Z_{ab} = first liquefiable layer thickness per Hutabarat and Bray [9] definition.

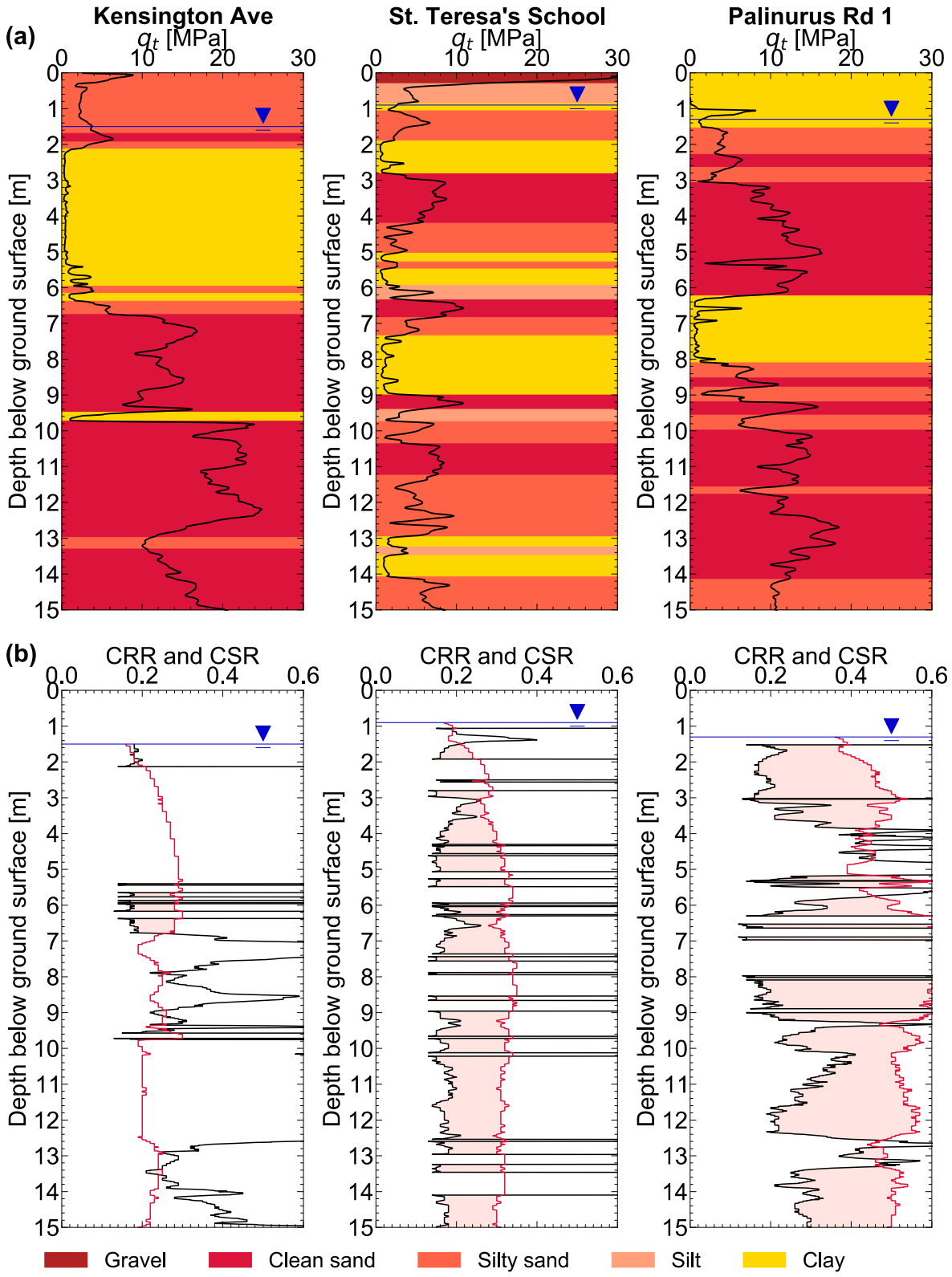

Fig. 14. Soil profiles of partially stratified silty soil sites (Kensington Ave and St. Teresa's School) and thick, clean sand site (Palinurus Rd 1) without ejecta for the Feb 2011 earthquake: (a) their corrected tip resistance (q_t) traces are shown in black with I_c-based layers colored, and (b) Boulanger and Idriss [26] cyclic resistance ratio (CRR, traces in black) and cyclic stress ratio (CSR, traces in red) adjusted for $M_w = 7.5$ and $\sigma'_{vo} = 1$ atm with $FS_L < 1$ layers shaded.

total of 6 m of non-liquefiable soil in the top 10 m (1.6-, 0.5-, and 3.8-m thick layers at respective depths of 1.5, 4.3, and 6.0 m) and a 1.3-m thick layer of clean sand between the two shallower layers of non-liquefiable soil.

Liquefaction indices are based on CPT measurements, but there are challenges in characterizing stratified silty soil deposits with the CPT due to the smearing of measurements (zone of influence > layer thickness) and the tip resistance of stiff sand within softer, more compressible

layers not being fully mobilized [36–38]. Additionally, most of the database used to develop the CPT-based liquefaction triggering procedures is comprised of case histories from sites with clean sand deposits and sand deposits with up to 35% of non-plastic fines. Finally, evidence suggests the stratified silty sites can have partially saturated soil layers over a considerable depth just below the estimated groundwater levels, which can increase the liquefaction resistance of shallow liquefiable soil layers [17,37].

5.3.2. Clean sand sites

Six strongly shaken, thick, clean sand sites did not produce ejecta in the Canterbury earthquakes (Table 3 and Fig. 14, and Fig. S3 in supplementary material). These sites are in the NE geologic quadrant, apart from the Palinurus Rd 1 site in the SE quadrant. The $PGA_{6.1}$ and site characteristics for the Feb 2011 earthquake vary from site to site (Table 3). LSN and LPI correctly estimate the severity of liquefaction-induced damage for most of these no-ejecta sites. The exceptions to this trend are observed for the Palinurus Rd 1 site (LSN = 37 and LPI = 30 indicate severe-to-extreme damage) and the Armagh St site (LPI = 6 indicates minor damage). The L_D-C_R chart correctly estimates the severity of ejecta-induced settlement at the Rawhiti Domain and Lakewood Dr sites but overestimates it slightly at the Keers Rd and Armagh St sites and significantly at the Palinurus Rd 1 and Tonks St sites (Table 3).

Of the six sites, the Palinurus Rd 1 site has the largest number of layers with contrasting permeabilities (Fig. 14a). The non-liquefiable soil in a 6.2–8.1 m depth range at the Palinurus Rd 1 site has the potential to obstruct the upward flow of water from the underlying liquefiable soil [9]. The Armagh St site has a relatively deep groundwater table (3.5 m) and a nearly continuous non-liquefiable soil layer extending from the ground surface to a depth of about 6 m. It overlies a layer of liquefiable sand that extends to a depth of 15 m. The long vertical distance from the top of the liquefiable layer to the ground surface (i.e., thick crust) inhibits the upward flow of liquefied material. At the Rawhiti Domain and Keers Rd sites, the groundwater tables are shallow but the tip resistances of the clean sand layers below the groundwater tables are high (15–25 MPa) with CRR > CSR throughout nearly the entire soil profiles. The Tonks St site has a relatively deep groundwater table (3.3 m) and contains a continuous clean sand layer from the bottom of the crust to a depth of 8.4 m with an average q_t of 16 MPa and CRR > CSR. At the Lakewood Dr site, the groundwater table is deep (3.0 m), and the vertical continuity of a clean sand layer with CRR > CSR is interrupted by layers of lower permeabilities in a depth range from 3.8 m to 5.6 m wherein a 0.3-m thick non-liquefiable layer overlies a 1.2-m thick sand layer with CRR < CSR. Crusts at these thick, clean sand sites are not exclusively comprised of primarily low-permeability or primarily high-permeability soil.

6. Conclusion

The Mijic et al. [13] liquefaction ejecta database was examined to identify general trends associated with the severity of ejecta-induced settlement and to evaluate the efficacy of liquefaction-induced damage indices such as LPI, LSN, and L_D-C_R, as well as the Ishihara [8] boundary curves. In the 235-case-history database, 69% of the sites are characterized by thick, clean sand deposits, 25% of the sites are characterized by stratified silty soil deposits, and 6% of the sites are gravel-dominated deposits. The key insights from this study are:

- Liquefaction ejecta occurred in all four main Canterbury earthquakes. The severity of the ejecta-induced settlement varied from site to site and from earthquake to earthquake. The Feb 2011 earthquake produced the most severe and frequent ejecta-induced settlement, whereas the Sep 2010 earthquake produced the least severe and frequent ejecta-induced settlement. The ejecta-induced settlement ranged from 0 mm to 155 mm for the Feb 2011 earthquake and from 0 mm to 40 mm for the Sep 2010 earthquake. The ejecta-induced settlement ranges for the Jun 2011 and Dec 2011 earthquakes were 0–105 mm and 0–120 mm, respectively.
- Ejecta were not generated at these sites by the Jun 2011 or Dec 2011 earthquake if eecta were not generated by the Feb 2011 earthquake. Additionally, ejecta did not occur in the Sep 2010 earthquake at 86% of the sites that produced ejecta in the Jun 2011 earthquake even though their $PGA_{6.1}$, groundwater depths, and crust and first liquefiable layer thicknesses did not differ significantly. A strong correlation between the Jun 2011 ejecta-induced settlement and the Feb 2011 ejecta-induced settlement suggests the Feb 2011 earthquake-induced liquefaction ejecta severely damaged the land, which helped the liquefied soil at depth to migrate more easily to the ground surface in the Jun 2011 earthquake.
- Sites with $PGA_{6.1} \leq 0.20$ *g* produced ≤ 15 mm (typically zero) of ejecta-induced settlement regardless of their soil profile characteristics. Sites with silty material in the top 10 m of the soil profile typically produced none-to-minor ejecta-induced settlement for $PGA_{6.1} \leq 0.40$ *g*, whereas thick, clean sand sites tended to experience more severe ejecta-induced settlement. The severity of ejecta at thick, clean sand sites increased as $PGA_{6.1}$ increased, especially when $PGA_{6.1}$ exceeded 0.40 *g*.
- Nearly all case histories with severe-to-extreme ejecta (97%) have thick, clean sand deposits. In the Feb 2011, Jun 2011, and Dec 2011 earthquakes, severe-to-extreme ejecta were formed under $PGA_{6.1}$ = 0.35–70 *g*, 0.24–0.44 *g*, and 0.33–0.37 *g*, respectively. No sites produced severe-to-extreme ejecta in the Sep 2010 earthquake even though $PGA_{6.1}$ ranged from 0.22 *g* to 0.40 *g*.
- When $PGA_{6.1}$ exceeded 0.30 *g* in the Jun 2011 earthquake, sites with shallower groundwater tables produced more ejecta-induced settlement than sites with deeper groundwater tables. Similarly, the ejecta-induced settlement tended to increase with the decreasing crust thickness for the Jun 2011 earthquake and $PGA_{6.1} > 0.30$ *g*. There was a moderate tendency for the ejecta-induced settlement to increase with increasing thickness of the first liquefiable soil layer in the Feb 2011 earthquake when $PGA_{6.1}$ exceeded 0.40 *g*.
- The Ishihara [8] boundary curves often overestimated liquefaction-induced ground damage for the no-ejecta case histories. This trend was most prominent for the Sep 2010 earthquake and least prominent for the Feb 2011 earthquake.
- In general, LPI and LSN underestimated the severity of non-zero ejecta at thick, clean sand sites and overestimated it at stratified silty soil sites. This systematic misestimation of liquefaction effects highlights the importance of system-response effects and the need for their incorporation in the liquefaction evaluation procedures.
- The L_D-C_R chart outperformed LPI and LSN at stratified silty sites without ejecta (TPR = 91% compared to 69% and 56%, respectively) and at thick, clean sand sites with severe-to-extreme ejecta (TPR = 64% compared to 14% and 18%, respectively). This underscores the importance of incorporating post-shaking hydraulic mechanisms in the formulation of liquefaction-induced damage indices.
- Residential properties with ground surface elevations higher than those of adjacent roads often manifested less ejecta than the roads. This likely occurred due to the roads having thinner crusts with more defects compared to the residential properties.
- Six strongly shaken thick, clean sand sites did not produce ejecta in any of the four main Canterbury earthquakes. They typically had thick clean sand layers with high tip resistances (CRR > CSR), thick non-liquefiable crusts, or deeper non-liquefiable layers overlying liquefiable layers with CRR < CSR. At strongly shaken stratified silty soil sites, the presence of multiple soil layers of contrasting permeabilities and liquefaction susceptibilities abated the manifestation of liquefaction at the ground surface.

Although important insights can be gleaned from the examination of these field case histories, there are limitations to consider. There is uncertainty in each of the parameters available in the database. The ejecta-

induced settlement used in the analysis of the database represents the best estimate of the ejecta-induced settlement for each case history based on the representative settlement assessment area(s) for a site. There were multiple assessment areas for each site to investigate the variability. Each site was centered at a selected CPT location, and radial areas of 10 m, 20 m, and 50 m were investigated, with assessment areas being an open field, residential area with patches of an open area, or road. It is assumed a CPT is representative of a settlement assessment area even though ejecta may not have been generated close to it. The spatial variability in soil conditions can be high in areas of Christchurch with complex depositional environments. Consequently, the CPT parameters (q_c and I_c) and the CPT-based indices (LPI, LSN, and L_D-C_R) and definitions (the first liquefiable layer and crust thicknesses) may not best describe the soil profile conditions that resulted in the estimated ejecta-induced settlement. The ejecta-induced settlement estimates are affected by the size of the assessment area and the spatial distribution of ejecta across the assessment area, both of which can differ from site to site. The quality of the photographs and LiDAR survey data also affects the ejecta-induced settlement estimates. There is also uncertainty in the PGA and groundwater depth estimates. Nevertheless, the liquefaction ejecta database provides a unique set of data for the analysis of the occurrence and effects of ejecta.

The liquefaction ejecta database can be improved by adding case histories for 20–30 stratified silty soil sites in Christchurch to balance the number of clean sand sites. It would also benefit from being complemented with case histories from other earthquakes in other geographic regions. It is essential that direct, reliable measurements of intact ejecta are taken after future earthquakes (e.g., using terrestrial LiDAR or structure-from-motion photogrammetry) and CPTs are advanced to best capture the soil profile that contributed to the observed spatial distribution of ejecta. Nonlinear effective stress analyses of the sites in the database can also improve our understanding of the differing responses of the sites.

Declaration of competing interest

The authors declare that they have no known competing financial interests or personal relationships that could have appeared to influence the work reported in this paper.

Data availability

The data analyzed in this study are part of the database previously published by the authors and referenced in this paper.

Acknowledgments

This research was supported by the U.S. Geological Survey (USGS), Department of Interior [grant number G20AP00079], and by the U.S. National Science Foundation (NSF) [grant number CMMI-1956248]. The views and conclusions contained in this document are those of the authors and should not be interpreted as necessarily representing the official policies, either expressed or implied, of the U.S. Government. Additional support was provided by the Faculty Chair in Earthquake Engineering Excellence at UC Berkeley and by Tonkin and Taylor Ltd. (T + T), New Zealand. Penn State Harrisburg supported the open-access publication of this paper. We thank Sjoerd van Ballegooy of T + T for helping us develop the ejecta database and for sharing his expertise. We also thank Michael Riemer of UC Berkeley and Misko Cubrinovski of the Univ. of Canterbury for providing feedback on this research.

Appendix A. Supplementary data

Supplementary data to this article can be found online at https://doi.org/10.1016/j.soildyn.2023.108267.

References

[1] Cubrinovski M, Bradley B, Wotherspoon L, Green R, Bray J, Wood C, et al. Geotechnical aspects of the 22 February 2011 Christchurch earthquake. Bull N Z Soc Earthq Eng 2011;44(4):205–26. https://doi.org/10.5459/bnzsee.44.4.205-226.

[2] Green RA, Cubrinovski M, Wotherspoon L, Allen J, Bradley BA, Bradshaw A, Bray JD, Winkley A. Geotechnical aspects of the Mw 6.2 2011 Christchurch, New Zealand earthquake. Oakland, CA, USA: 2012 Annual Congress of the Geo-institute of ASCE; 2012. p. 25–9. Mar 2012.

[3] Rogers N, van Ballegooy S, Williams K, Johnson L. Considering post-disaster damage to residential building construction - is our modern building construction resilient? 6th International Conference on Earthquake Geotechnical Engineering. 2015. Christchurch, New Zealand.

[4] Beyzaei CZ, Bray JD, van Ballegooy S, Cubrinovski M, Bastin S. Depositional environment effects on observed liquefaction performance in silt swamps during the Canterbury earthquake sequence. Soil Dynam Earthq Eng 2018;107:303–21. https://doi.org/10.1016/j.soildyn.2018.01.035.

[5] Iwasaki T, Tatsuoka F, Tokida K, Yasuda S. A practical method for assessing soil liquefaction potential based on case studies at various sites in Japan. In: Proceedings of the 2nd international conference on microzonation. Washington, DC: National Science Foundation; 1978. p. 885–96.

[6] van Ballegooy S, Malan P, Lacrosse V, Jacka ME, Cubrinovski M, Bray JD, O'Rourke TD, Crawford SA, Cowan H. Assessment of liquefaction-induced land damage for residential Christchurch. Earthq Spectra 2014;30(1):31–55. https://doi.org/10.1193/031813EQS070M.

[7] Ishihara K, Yoshimine M. Evaluation of settlements in sand deposits following liquefaction during earthquakes. Soils Found 1992;32(1):173–88. https://doi.org/10.3208/sandf1972.32.173.

[8] Ishihara K. Stability of natural deposits during earthquakes. Proceedings of the 11th international conference on soil mechanics and foundation engineering, vols. 321–376. London, UK: International Society of Soil Mechanics and Foundation Engineering; 1985.

[9] Hutabarat D, Bray JD. Estimating the severity of liquefaction ejecta using the cone penetration test. J. Geotech. Geoenviron. Eng. ASCE 2022;148(3):04021195. https://doi.org/10.1061/(ASCE)GT.1943-5606.0002744.

[10] Bray JD, Olaya FR. 2022 H. Bolton seed memorial lecture: evaluating liquefaction effects. J Geotech Geoenviron Eng 2023;149(8). https://doi.org/10.1061/JGGEFK.GTENG-11242.

[11] Hutabarat D, Bray JD. Effective stress analysis of liquefiable sites to estimate the severity of sediment ejecta. J. Geotech. Geoenviron. Eng. ASCE 2021;147(5). 10.1061/(ASCE)GT.1943-5606.0002503.

[12] Bray JD, Macedo J. 6th Ishihara lecture: simplified procedure for estimating liquefaction-induced building settlement. Soil Dynam Earthq Eng 2017;102:215–31.

[13] Mijic Z, Bray JD, van Ballegooy S. Liquefaction ejecta case histories for 2010-11 Canterbury earthquakes. ISSMGE J.Geoeng. Case Histories 2022;6(3):73–93. https://doi.org/10.4417/IJGCH-06-03-04.

[14] Tonkin and Taylor, Ltd. (T + T). Tonkin and Taylor geotechnical database: Canterbury maps (database). 2015. Retrieved from https://canterburygeotechnicaldatabase.projectorbit.com/.

[15] Land Damage Assessment Team (LDAT). LDAT reports data entry (database). 2021. Retrieved from, https://tracker.projectorbit.com/Sites/LDAT/EQCFieldReportFormExtra.aspx.

[16] Robertson PK. Interpretation of cone penetration tests – a unified approach. Can Geotech J 2009;46:1337–55.

[17] Cubrinovski M, Rhodes A, Ntritsos N, van Ballegooy S. System response of liquefiable deposits. Soil Dynam Earthq Eng 2019;124:212–29. https://doi.org/10.1016/j.soildyn.2018.05.013.

[18] Zhang G, Robertson PK, Brachman RWI. Estimating liquefaction-induced ground settlements from CPT for level ground. Can Geotech J 2002;39:1168–80. https://doi.org/10.1139/T02-047.

[19] Ang AS, Tang WH. Probability concepts in engineering: emphasis on applications to civil and environmental engineering. second ed. Wiley; 2007.

[20] Schober P, Boer C, Schwarte LA. Correlation coefficients: appropriate use and interpretation. Anesth Analg 2018;126(5):1763–8. https://doi.org/10.1213/ANE.0000000000002864.

[21] Forthofer RN, Lee ES, Hernandez M. Biostatistics. In: Descriptive methods. second ed. Academic Press; 2007. p. 3. https://doi.org/10.1016/B978-0-12-369492-8.50008-X.

[22] Bradley B, Hughes M. Conditional peak ground accelerations in the Canterbury earthquakes for conventional liquefaction assessment. New Zealand: Technical Report prepared for the Department of Building and Housing; 2012.

[23] Bradley BA, Hughes M. Conditional peak ground accelerations in the Canterbury earthquakes for conventional liquefaction assessment: Part 2. New Zealand: Technical Report prepared for the Ministry of Business, Innovation and Employment; 2012.

[24] Idriss IM, Boulanger RW. Soil liquefaction during earthquakes. EERI Monograph MNO-12. 2008.

[25] Ioannides JT. CLiq v.3.0.3.2 – CPT soil liquefaction software. Greece: Geologismiki; 2019.

[26] Boulanger RW, Idriss IM. CPT-based liquefaction triggering procedure. J Geotech Geoenviron Eng 2016;142(2):04015065. https://doi.org/10.1061/(asce)gt.1943-5606.0001388.

[27] de Greef J, Lengkeek HJ. Transition and thin layer corrections for CPT based liquefaction analysis. In: Proceedings of the 4th international symposium on cone penetration testing (CPT'18); 2018. p. 21–2. Jun, 2018, Delft, The Netherlands.
[28] Obermeier SF. The New Madrid earthquakes; an engineering-geologic interpretation of relict liquefaction features. US Geological Survey Professional Paper 1336-B; 1989.
[29] Obermeier SF. Use of liquefaction-induced features for paleoseismic analysis. Eng Geol 1996;44:1–76.
[30] Audemard FA, de Santis F. Survey of liquefaction structures induced by recent moderate earthquakes. Bull Int Assoc Eng Geol 1991;44:5–16.
[31] Maurer BW, Green RA, Cubrinovski M, Bradley BA. Evaluation of the liquefaction potential index for assessing liquefaction hazard in Christchurch, New Zealand. J Geotech Geoenviron Eng 2014;140(7):1–11. https://doi.org/10.1061/(asce)gt.1943-5606.0001117. 04014032.
[32] Hutabarat D, Bray JD. Seismic response characteristics of liquefiable sites with and without sediment ejecta manifestation. J. Geotech. Geoenviron. Eng. ASCE 2021; 147(6). 10.1061/(ASCE)GT.1943-5606.0002506.
[33] Canterbury Geotechnical Database (CGD). LiDAR and digital elevation models. 2015. Map Layer CGD0500 - 20 July 2015, retrieved 25 July 2022 from, https://canterburygeotechnicaldatabase.projectorbit.com/.
[34] Canterbury Geotechnical Database (CGD). Aerial photography. 2012. Map Layer CGD0100 - 1 June 2012, retrieved 25 July 2022 from, https://canterburygeotechnicaldatabase.projectorbit.com/.
[35] Canterbury Geotechnical Database (CGD). Vertical ground surface movements, map layer CGD0600 – 23 July 2012, retrieved 25 July 2022 from. https://canterburygeotechnicaldatabase.projectorbit.com/.
[36] Ahmadi MM, Robertson PK. Thin-layer effects on the CPT q_c measurement. Can Geotech J 2005;42:1302–17. https://doi.org/10.1139/T05-036.
[37] Beyzaei CZ, Bray JD, Cubrinovski M, Bastin S, Stringer M, Jacka M, van Ballegooy S, Riemer M, Wentz R. Characterization of silty soil thin layering and groundwater conditions for liquefaction assessment. Can Geotech J 2020;57(2): 263–76. https://doi.org/10.1139/cgj-2018-0287.
[38] Mijic Z, Bray JD, Riemer MF, Rees SD, Cubrinovski M. Cyclic and monotonic simple shear testing of native Christchurch silty soil. Soil Dynam Earthq Eng 2021;148: 106834. https://doi.org/10.1016/j.soildyn.2021.106834.